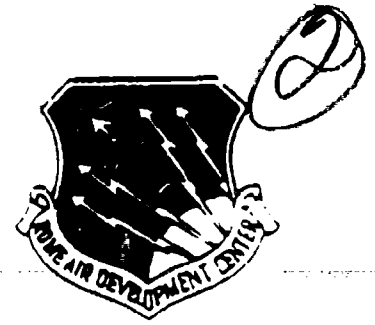


AD-A237 012



RADC-TR-90-259
Final Technical Report
October 1990

TROPOSPHERIC SCATTER PROPAGATION AT 5 AND 16 GHz: RESULTS FOR A 161 KM PATH

Dartmouth College

Robert K. Crane



APPROVED FOR PUBLIC RELEASE; DISTRIBUTION UNLIMITED.

Rome Air Development Center
Air Force Systems Command
Griffiss Air Force Base, NY 13441-5700

91 0 14 039

91-02163

This report has been reviewed by the RADC Public Affairs Division (PA) and is releasable to the National Technical Information Service (NTIS). At NTIS it will be releasable to the general public, including foreign nations.

RADC-TR-90-259 has been reviewed and is approved for publication.

APPROVED: *Uve H. W. Lammers*

UVE H. W. LAMMERS
Project Engineer

APPROVED: *John K. Schindler*

JOHN K. SCHINDLER
Director of Electromagnetics

FOR THE COMMANDER:

James W. Hyde III

JAMES W. HYDE III
Directorate of Plans & Programs

If your address has changed or if you wish to be removed from the RADC mailing list, or if the addressee is no longer employed by your organization, please notify RADC (EECP) Hanscom AFB MA 01731-5000. This will assist us in maintaining a current mailing list.

Do not return copies of this report unless contractual obligations or notices on a specific document require that it be returned.

REPORT DOCUMENTATION PAGE

Form Approved
OMB No. 0704-0188

Public reporting burden for this collection of information is estimated to average 1 hour per response, including the time for reviewing instructions, searching existing data sources, gathering and maintaining the data needed, and completing and reviewing the collection of information. Send comments regarding this burden estimate or any other aspect of this collection of information, including suggestions for reducing this burden, to Washington Headquarters Service, Directorate for Information Operations and Reports, 1215 Jefferson Davis Highway, Suite 1204, Arlington, VA 22202-4302, and to the Office of Management and Budget, Paperwork Reduction Project (0704-0188), Washington, DC 20503.

1. AGENCY USE ONLY (Leave Blank)		2. REPORT DATE October 1990		3. REPORT TYPE AND DATES COVERED Final Jun 88 - Jun 89	
4. TITLE AND SUBTITLE TROPOSPHERIC SCATTER PROPAGATION AT 5 AND 16 GHz: RESULTS FOR A 161 KM PATH				5. FUNDING NUMBERS C - F30602-88-D-0027 PE - 63789F PR - 478T TA - 00 WU - P1	
6. AUTHOR(S) Robert K. Crane					
7. PERFORMING ORGANIZATION NAME(S) AND ADDRESS(ES) Dartmouth College Thayer School of Engineering Hanover NH 03755				8. PERFORMING ORGANIZATION REPORT NUMBER	
9. SPONSORING/MONITORING AGENCY NAME(S) AND ADDRESS(ES) Rome Air Development Center (EECP) Hanscom AFB MA 01731-5000				10. SPONSORING/MONITORING AGENCY REPORT NUMBER RADC-TR-90-259	
11. SUPPLEMENTARY NOTES RADC Project Engineer: Uve Lammers/EECP/(617) 377-3193					
12a. DISTRIBUTION/AVAILABILITY STATEMENT Approved for public release; distribution unlimited.				12b. DISTRIBUTION CODE	
13. ABSTRACT (Maximum 200 words) Simultaneous transmission loss measurements were made at Ku-band (16 GHz) and C-band (5 GHz) on a 161 km tropospheric scatter link between Prospect Hill in Waltham, MA and Mt. Tug in Enfield, NH. The experiment was conducted to demonstrate the feasibility of using the higher frequency for scatter communication. Between April and September, 1987, two-frequency observations were obtained during a variety of weather conditions. Clear weather measurements were made to generate transmission loss estimates for comparison with tropospheric scatter model predictions. Observations during times with precipitation were made to assess the anticipated problems of an excess of transmission loss due to attenuation by rain at the higher frequency and an increase in delay spread due to scattering by rain.					
14. SUBJECT TERMS Troposcatter Propagation, Transmission Loss, Multipath Delay Spread, C-band, Ku-band, Tactical Troposcatter				15. NUMBER OF PAGES 48	
				16. PRICE CODE	
17. SECURITY CLASSIFICATION OF REPORT UNCLASSIFIED		18. SECURITY CLASSIFICATION OF THIS PAGE UNCLASSIFIED		19. SECURITY CLASSIFICATION OF ABSTRACT UNCLASSIFIED	
				20. LIMITATION OF ABSTRACT UL	

TROPOSPHERIC SCATTER PROPAGATION AT 5 AND 16 GHz:

RESULTS FOR A 161 km PATH

SUMMARY OF RESULTS

A two-frequency tropospheric scatter (troposcatter) propagation experiment was conducted in cooperation with Rome Air Development Center (RADC) personnel at Hanscom AFB, MA. The object of the experiment is to investigate the feasibility of the Ku frequency band for tactical troposcatter communications. The measurement program was designed to verify the predictions of the standard models for troposcatter propagation and to explore the potential limits to link reliability that many system designers attribute to attenuation by rain.

At the end of two years of experimentation at Ku-band and one year at C-band, the following results have been obtained:

- Three different propagation modes have been detected, turbulent volume scatter, rain scatter and ducting via elevated layers.
- The most common propagation mode is turbulent volume scatter.
- The standard troposcatter models available in the general literature or recommended by the International Radio Consultative Committee (CCIR) of the International Telecommunications Union (ITU) forecast the observed median signal levels with an error of less than 3 dB.
- The standard models can be improved by using a turbulent volume scattering model in place of the thin scattering layer assumption of the standard models.
- The prediction error for the turbulent volume scatter model is less than 1 dB if turbulent volume scatter is the active propagation mode and the prediction is based on simultaneous C-band measurements.
- The years of experience in the design and operation of C-band troposcatter systems accumulated by the Air Force may be used for the successful design of Ku-band

troposcatter systems by frequency scaling to Ku-band on the basis of the turbulent volume scatter model.

- The available bandwidth for a Ku-band link will differ little from the bandwidth of a C-band system employing antennas with the same gain as the Ku-band system.
- Rain scatter will affect (improve) the performance of a Ku-band system by increasing the median signal level for a large fraction of the time with rain.
- Rain scatter will not significantly reduce the available link bandwidth.
- Attenuation by rain did not significantly reduce link availability (but only moderate rain rates have been observed to date).
- The rain scattered Ku-band signal ranged from within 1 dB of the unattenuated signal level to 10 dB above the signal level predicted from simultaneous C-band measurements using the bistatic radar equation.
- The C-band system experienced significant signal losses (greater than 10 dB in the level of signals averaged for 2 minutes) in times of rain when the rain scattered signal was below the expected signal level for turbulent volume (clear weather) scatter.
- The C-band signal depression appeared to be caused by a reduction in the level of the turbulent volume scattering during times with rain, a reduction also evident at Ku-band.
- The lowest signal levels were detected during times with rain but these signal levels were produced by turbulent volume scattering with a reduced scattering intensity, C_n^2 .
- Enhanced signal levels at Ku-band not associated with rain on the path were also observed.
- The enhanced signals were accompanied by a significant reduction in the fade rate and an increase in channel bandwidth (reduction in delay spread).
- These enhanced Ku-band signals were accompanied by significantly depressed C-band signal levels.

- The slow fading was observed simultaneously on both channels.
- A possible explanation for the enhanced signal conditions is coupling via elevated ducting layers.

These results were obtained from a limited set of observations but the conclusions can be drawn because sufficient data were available from the two-frequency observations and the delay spread measurements at Ku-band to identify the propagation mode for each data set.

A detailed description of the results of the experiment obtained to date are presented in a paper prepared for submission to the IEEE Transactions on Antennas and Propagation. The paper is appendix A of this report.

Eleven data sets of sufficient length for analysis were obtained on nine different days in 1987. The analyses described in the paper (appendix A) were performed for each of the data sets. The results for each data set are presented in the figures in appendix B.

Additional work that needs to be done:

- The results obtained to date are for a large, 29 ft., transmit antenna which is not representative of any antenna to be used in a practical system. Observations at Ku-band should be made with 3 ft. transmit and receive antennas.
- The data on available bandwidth are significantly affected by the small beamwidths associated with the large transmit antenna especially during periods with rain scatter.
- The modeled delay spreads (impulse response for the channel) are 12 nsec for turbulent volume scatter and 16 nsec for rain scatter when using the 29 ft. transmit antenna. A pseudorandom sequence (PRN code) with a significantly higher bit rate (than the current 12.5 MHz) must be used to resolve the details of the delay spread profile. A 400 MHz bit rate would have a 2.5 nsec resolution which is adequate to resolve the modeled delay spread.
- Simultaneous delay spread observations are needed at C-band to aid in identifying and classifying enhanced elevated ducting layer propagation conditions.

For	<input checked="" type="checkbox"/>
&I	<input type="checkbox"/>
ed	<input type="checkbox"/>
tion	

Description/	
Availability Codes	
Avail and/or	
Special	

Dist
A-1

- A significantly larger data base must be acquired for propagation model evaluation. A viable procedure for troposcatter system design for frequencies above 5 GHz will need statistical information on the separate propagation modes. The experience at C-band can only be used for extrapolation to higher frequencies for the turbulent volume scatter mode. More data are needed for rain and elevated ducting layers.
- Rain should produce attenuation in excess of 1 dB at Ku-band on the Prospect Hill to Mt. Tug path for 12.7 percent of an average year. The 33 hours of observations in rain account for approximately 3 percent of the time with rain. The maximum rain rate observed during the measurement campaign was less than 10 mm/h. More observations are needed to explore fully the impact of rain on a Ku-band troposcatter link.
- A reliable, automated method for establishing the propagation mode is needed. We are currently modifying the computer programs to obtain mean differential Doppler data from the two-frequency carrier measurements. Rain should produce a differential Doppler signature that is different from the signature for turbulent volume scatter and allow the separation of those modes.

TROPOSPHERIC SCATTER PROPAGATION AT 5 AND 16 GHz:

PRELIMINARY RESULTS FOR A 161 km PATH

Robert K. Crane

Thayer School of Engineering
Dartmouth College, Hanover, NH 03755

ABSTRACT

Simultaneous transmission loss measurements were made at Ku-band (16 GHz) and C-band (5 GHz) on a 161 km tropospheric scatter link between Prospect Hill in Waltham, MA and Mt. Tug in Enfield, NH. The experiment was conducted to demonstrate the feasibility of using the higher frequency for scatter communication. Between April and September, 1987, two-frequency observations were obtained during a variety of weather conditions. Clear weather measurements were made to generate transmission loss estimates for comparison with tropospheric scatter model predictions. Observations during times with precipitation were made to assess the anticipated problems of an excess of transmission loss due to attenuation by rain at the higher frequency and an increase in delay spread due to scattering by rain.

The sample medians of the transmission loss values for twelve hours of observation during periods with normal fade rates and clear weather conditions were 157 dB at 15.73 GHz and 144 dB at 4.95 GHz, values within 3 dB of the predictions of the CCIR transmission loss prediction method I when attenuation by gaseous absorption is included in the calculations and within 1 dB of the predictions of a turbulent volume scattering model. The limited number of clear weather measurements made during the 1987 observation campaign were not enough to provide a statistical basis for model validation but were enough to test the frequency dependence of the model predictions for transmission loss. The frequency dependence of the observations were in agreement with the turbulent volume scattering model predictions. Sixty-six percent of the data, 33 hours, were obtained during periods with precipitation in the vicinity of the troposcatter path. At no time during rainy conditions on the path did the signal drop below the receiver noise level or show a significant increase in delay spread. The highest Ku-band signal levels were recorded during times with rain as were the lowest and the median Ku-band signal levels for rainy conditions were higher than for clear weather conditions. By way of contrast, the C-band median signal levels were lower for rain than for clear weather conditions. Enhanced clear weather Ku-band signal levels accompanied very slow fading and depressed C-band signal levels were detected during ten percent of the observations.

1. INTRODUCTION

Simultaneous transmission loss measurements were made at Ku-band (15.73 GHz) and C-band (4.95 GHz) on a 161 km tropospheric scatter (troposcatter) link between a

transmitter site on Prospect Hill in Waltham, MA and a receiver site on Mt. Tug in Enfield, NH. The experiment was conducted to demonstrate the feasibility of employing frequencies in the Ku-band for troposcatter communication. The C-band observations were obtained to provide a reference channel with known transmission loss characteristics. Delay spread measurements were made at Ku-band to assist in characterizing the channel. The two-frequency measurements were obtained during a variety of weather conditions. Clear weather observations were used to generate transmission loss estimates for comparison with troposcatter propagation loss model predictions. Observations during times with precipitation were conducted to assess the anticipated problems of excess transmission loss due to attenuation and increased delay spread due to scattering by rain. By design, the measurements were made primarily during periods with rain; roughly 70 percent of the observations were for rainy conditions somewhere on the path.

The results derived from the observations during the 1987 measurement campaign were 1) the troposcatter field strengths at 16 GHz were higher than predicted (transmission loss values were lower than expected) using the standard CCIR model (method I when corrected for gaseous absorption [CCIR, 1986]) and simultaneous 5 GHz observations, 2) the standard model should be revised to include attenuation by gaseous absorption and employ scattering by turbulence for predictions at frequencies above 5 GHz, 3) enhanced 16 GHz signal levels accompanied by very slow fading were occasionally observed during clear weather conditions and 4) the occurrence of rain on the path generally led to signal level increases of as much as 25 dB over no rain conditions for rain rates less than 10 mm/h. The last point is important because it contradicts the assumptions usually made when considering a move to higher frequencies. It is also important in the assessment of the potential for interference between radio frequency (RF) systems sharing the same frequencies (co-channel interference). The occurrence of clear weather signal levels enhanced by 15 dB or more is also important for interference modeling.

The general background for the experiment is presented in section 2, the experiment is described in section 3, the analysis of measurements and a comparison with model predictions is presented in section 4.

2. BACKGROUND

Troposcatter is used for communication by the military and by some commercial operators for applications such as communication with off-shore oil rigs. C-band frequencies are currently used for troposcatter systems but operation at higher frequencies could be advantageous for tactical communications because the antenna size needed to produce a given antenna gain is smaller at the higher frequency and the models for troposcatter transmission loss suggest a strong dependence of signal level on antenna gain. Smaller antennas would be easier to mount on vehicles and to transport from one location to the next. Conventional wisdom argues against the use of the higher frequencies because of the expected decrease in link reliability and available bandwidth during periods with rain. This measurement program was initiated to quantify the problems associated with a move to higher frequencies.

A number of troposcatter experiments were conducted during the 1950s and 1960s at frequencies up through 10 GHz. The Central Radio Propagation Laboratory (CRPL) of the National Bureau of Standards collected data from experiments made worldwide and summarized the results of the measurements with an empirical model for the estimation of the cumulative distribution of annual hourly median transmission loss as a function of frequency and path geometry [Rice et al., 1965]. Hourly median values were used in the analysis because they were easy to determine with available equipment and they provided a reasonably robust estimate of the average signal level, an estimate which was not affected by transient events such as scattering by passing aircraft. If sufficient data were available, the statistics of the hourly median signal levels would not differ from the statistics of averages or median levels calculated for different time intervals.

Most of the observations included in the CRPL statistical analysis were obtained at frequencies below 1 GHz. A few troposcatter transmission loss experiments have been conducted at frequencies above 10 GHz during the last 20 years [Abel, 1972; Olsen and Lammers, 1978; Vilar et al., 1988]. Except for the work of Abel, these observations were made to investigate the high level field strengths important for interference problems not the low level fields important for communication link reliability.

The majority of the observations available for transmission loss model development and model verification were made at frequencies below 1 GHz. For these measurements, the important localized variations in refractive index which cause the scattering needed for

communication take place within a single Fresnel zone with the result that the electromagnetic scattering process can be modeled by plane wave reflections from an ensemble of dielectric interfaces (or layers). At higher frequencies, the same refractive index variations will span a number of Fresnel zones and a different physical model must be invoked to describe the scattering process. A statistical approach to modeling the spatial correlations between the refractive index variations within the different Fresnel zones was developed by Tatarski [1961]. It was found to be useful for the estimation of the scattered signal levels and forms the basis for the turbulent volume scatter models.

Two different models have evolved for the prediction of the signal levels produced by scattering from the vertically thin but horizontally widespread turbulent volumes containing the refractive index fluctuations, the thin layer and the turbulent volume models [Crane, 1981]. The CRPL empirical prediction method was constrained to approximate the thin layer model. It forms the basis for the procedures recommended by the International Radio Consultative Committee (CCIR) for the design of troposcatter communication links [CCIR, 1986; 1988]. At frequencies above about 5 GHz, the empirical thin layer model is no longer adequate and a turbulent volume scattering model is needed for improved prediction accuracy. The transition from one scattering process to the other depends on the propagation geometry and the intensity and structure of the refractive index fluctuations in the scattering volume. A given path may exhibit the characteristics of layer scatter at one time and volume scatter at another. Unfortunately, in the recommendations of the CCIR for troposcatter system design, no reference is made to the volume scattering process although caution is advised in using the models at frequencies above 5 GHz. At 16 GHz, a path can only be characterized by the turbulent volume scatter process. A goal of this measurement program is to demonstrate the necessity of using the turbulent volume scattering model.

More than scattering by refractive index fluctuations is important in the modeling of link reliability at 16 GHz. Rain is known to attenuate signals at 16 GHz and, on the long paths employed for scatter links, rain attenuation may be severe. Abel [1972] noted a complete loss of signal for short periods during rain on a 210 km scatter link over the Rhine valley at 12 GHz. He also noted increases of up to 8 dB with respect to the clear weather scattered signal levels. Rain is an efficient scatterer and additional signal energy will be directed toward the receiver by rain scatter. These two effects, attenuation and scattering, counter each other. The conventional wisdom used in troposcatter system design is to stay away from the higher frequencies because rain attenuation will reduce the signal to levels not

useful for communication. A second goal of this program is to determine the validity of this conventional wisdom and establish the reliability of a link at Ku-band. A simple calculation suggests that rain may in fact cause signal level increases more often than signal losses. For a 200 km scatter path, the scattering angle will be about 1.4° producing a turbulent volume scattering cross section per unit volume at Ku-band (15.73 GHz) of $1.7 \times 10^{-8} \text{ m}^{-1}$ for a C_n^2 value of $10^{-15} \text{ m}^{-2/3}$ while, for the same path, rain at 10 mm/h will produce a scattering cross section per unit volume of $2 \times 10^{-5} \text{ m}^{-1}$, more than 30 dB higher. The additional attenuation through rain will generally be less than 30 dB with a net gain in signal strength in rain when compared with the signal levels received during clear weather conditions.

Duct propagation in elevated layers may also occur on troposcatter paths at higher frequencies. Such occurrences would be marked by increased median signal levels relative to the turbulent scatter, clear weather signal levels and by slower fading or signal fluctuation rates than for turbulent scatter [Crane, 1981]. Abel noted periods with as much as 30 to 40 dB increases in signal strength and much slower signal level variations. Vilar et al. [1988], in their short communication, noted the occurrence of enhanced signal levels relative to the clear weather long term median level due to all three propagation modes, rain scatter, turbulent volume scatter and ducting on an over water path at 11.6 GHz. Enhanced turbulent volume scatter will happen when increased refractive bending in the lower atmosphere decreases the scattering angle and thereby produces a higher scattering cross section per unit volume than normal. They identified the different propagation conditions by the observed fade rate [see also Crane, 1981].

3. THE EXPERIMENT

The troposcatter transmitters on Prospect Hill were operated and maintained by Rome Air Development Center (RADC) personnel at Hanscom AFB, MA. The 15.731 GHz Ku-band system used a 29 ft. steerable antenna. The antenna and transmitter were previously employed for troposcatter and ice scatter measurements on a long, 430 km path to a receiver site in Ottawa, Ontario, Canada [Olsen and Lammers, 1978]. The transmitted carrier signal could be phase modulated with a 1023 maximum-length pseudorandom sequence (PRN code) at a 12.5 MHz bit rate. The 4.95 GHz C-band system used a separate transmitter and feed on the same antenna. The C-band system employed a carrier without modulation. The carrier frequencies for the two systems were coherently derived

from the same master oscillator. At an early stage of the experiment it was hoped to defocus the antenna at 16 GHz to provide matched transmitter beams but this did not prove to be feasible. The final system used the full gain of the 29 foot aperture at each frequency. The characteristics of the transmitter systems are listed in Table 1.

Matched beamwidth receiver systems were constructed at Mt. Tug in Enfield NH [Levins, 1986; Sullivan, 1987]. The Ku-band system was fabricated from a wide-band channel probe (RAKE receiver) owned by the Air Force. The signals were synchronously detected with the in-phase and quadrature signals passed through 120 Hz bandwidth low-pass filters prior to analog-to-digital conversion and computer sampling. The C-band system was generally used to provide the phase reference for the Ku-band system but the signal phase reference channel could be switched. A correlation detector in the Ku-band receiver was used to sample sequentially up to twelve adjacent time steps (lags or taps) of the pseudorandom sequence. The receiver system was computer controlled to track the lag that produced the maximum output and sample three time lags before and eight after the time delay producing the maximum signal. In addition the power at each carrier frequency was sampled and recorded. The characteristics of the receiver system are also listed in Table 1.

The troposcatter path lies over a region that is relatively flat from the transmitter site to about 70 km from the transmitter with height variations in this area of less than 100 m. The remainder of the path has more terrain height variation with peak to valley changes of 400 m. The radio horizons are defined by obstacles (wooded hills) in the region with more height variation. The path profile for a $4/3$ effective earth radius is presented in Figure 1. The receive antennas were pointed just above the average radio horizon with their lower half power points directed at the terrain obstructions. The half power pattern for the dish antennas (the same for both frequencies) is depicted in the figure. The transmit antenna was nominally pointed at -0.05° which is toward the local radio horizon. Half the transmit beam is obstructed by the hill defining the local horizon. The pointing angle was selected to maximize the Ku-band received signal on a clear weather day without anomalous or extreme refractive conditions. Only the portions of the beams (within the half power antenna pattern in the great circle plane) above the horizon are displayed in the figure. The transmit patterns were not matched. The upper edge of the half power beams are labeled by frequency.

The scattering volumes as defined by the intersections of the half power beamwidths of the antenna patterns are indicated in the figure by cross-hatching. The scattering volume at

Ku-band is enclosed within the volume for C-band. The scattering volumes span a vertical thickness of 500 m at Ku-band and 700 m at C-band. The scattering volumes are long and thin with maximum horizontal extents of 32 km at Ku-band and 44 km at C-band. The horizontal widths of the scattering volumes are 340 m at Ku-band and 1070 m at C-band.

Horn antennas were mounted beside and above the dish antennas and could also be used for reception. Under computer control, the horn antennas, dish antennas, or noise diodes could be connected to the receiver via waveguide switches (coaxial switches at C-band). The noise diodes were used for periodic receiver calibration. A flexible sampling and data logging system was employed to record the in-phase and quadrature signals. The sampling rate was computer selectable but was usually set at 250 samples per second. The normal data recording mode entailed the calculation of an average for the power in each carrier and for each channel or lag (of 12) of the PRN code at Ku-band. The carrier and correlation detector channels were sampled sequentially in blocks of 100 to 200 samples per channel. To extend the dynamic range of the system, a computer controlled attenuator was placed in the first IF of each receiver. The attenuator settings were recorded with the power for selectable averaging intervals.

4. THE OBSERVATIONS

A sample observation set for a day with clear weather and normal fade rates is presented in Figures 2 through 5. The data were taken on August 3, 1987 at the times displayed in Figures 2 and 4. Figure 2 depicts the time series of received signal level normalized to a 30 watt transmitted carrier level (in dBm or transmission loss in dB). The received carrier power level values from the 120 Hz filters were averaged for 30 seconds for display and analysis for the figures. Shorter-term signal level variations were examined during several data runs on different days with clear weather conditions and found to have a Rayleigh distribution of signal level as expected for thin layer or turbulent volume scattering conditions [Stamboulis, 1987]. The 30 second or longer averaging intervals used for most of the data analysis were selected to remove the variations due to Rayleigh fading from the time series. The cumulative signal level distribution for the 30 second averages is shown in Figure 3. A straight line in this figure corresponds to a lognormal distribution. The slope of the line represents a standard deviation of the signal level of 4.2 dB. The median values for this data set are -99 dBm at 4.95 GHz and -107 dBm at 15.73 GHz. The receiver noise levels are -144 dBm and -146 dBm for the Ku-band and C-band

receivers respectively as indicated in Figure 2. The minimum signal-to-noise level during the observation period was 23 dB at Ku-band and 38 dB at C-band. The plotting scale is for a gaussian or normal probability distribution. The reduced variate is $(x-m)/S$ where x is the variate (power level in dBm), m is the mean value and S is the standard deviation.

The relative behavior of the channel at the two frequencies is depicted in Figures 4 and 5. Figure 4 presents the simultaneous differences in received signal levels (in dB) at the two frequencies. The signal-to-median levels were first calculated then their ratios were computed for display. The median signal levels used for this display are for all observations during the 1987 measurement campaign with clear weather conditions and normal fade rates. The figure displays the expected random variations in signal level. The number of independent samples, from the Rayleigh fading process that characterizes the short-term variations in received signal, used to estimate the 30 second power level values for the time series varied during the observation period. Two data gathering modes were employed, carrier sampling only and carrier samples plus sequential steps from twelve correlator lags. The latter mode of sampling reduced the number of samples available to estimate a value in the time series. The increase in variance of the time series estimates is evident in the periodic widening of the fluctuations between the Ku-band and C-band levels.

Figure 5 displays the power spectra of the signal level variations at each frequency for two averaging intervals, 30 and 120 seconds. Two power spectra are displayed for each frequency and averaging interval, spectra computed using the signal power values (Linear) and spectra computed using the received power levels in dB (Log). Because the low frequency components of the spectra are of interest in understanding the geophysical processes responsible for the scattered signals, windowing and zero-padding were not used in the preparation of the spectra. The log time series was adjusted prior to processing by subtracting the median level for the data set. The linear time series was obtained by exponentiation of the median adjusted values from the time series for the logarithm of the received signal. The spectral estimates presented in the figure are averages of 3 or 14 sequential FFTs of the 120 or 30 second average time series data respectively. Spectral averaging was employed to reduce the statistical uncertainties associated with spectral estimation. Thirty-two samples were used for each FFT. At 120 seconds per sample, this corresponds to a little over an hour of observations for each FFT in the averaged periodogram. Crane [1987] found that longer intervals could not be used if the time series is to be interpreted in terms of a spatial series.

At the frequencies employed for this experiment, received signal levels are proportional to the intensity of the refractive index fluctuations in the scattering volume. Using C_n^2 to represent the intensity of the turbulent fluctuations, the C_n^2 values change with the horizontal advection of the atmosphere through the scattering volume. If the scattering volume and observing time are small enough, the temporal changes in C_n^2 in the scattering volume should correspond to spatial changes in C_n^2 along a line in the direction of the mean wind at the height of the scattering volume. The one-dimensional spectrum of the refractive index fluctuations, $F(k)$ where the wavenumber $k = 2\pi/l$ with $l =$ wavelength, is modeled to have a $C_n^2 \propto k^{-5/3}$ behavior for three-dimensional turbulent fluctuations of the refractive index in the inertial subrange (spatial scales from 0.01 to 100 m responsible for the scattering of the electromagnetic signal [Crane, 1980]). At much larger spatial scales, scales greater than about 12 km, two-dimensional turbulent fluctuations in C_n^2 may also be modeled as having a $k^{-5/3}$ behavior [Crane, 1987]. The scattering volume for a single time delay (tap of the RAKE receiver) has dimensions of approximately 0.4 km in the vertical and 0.3 km across the path in the horizontal. Along the path, the horizontal dimension is about 30 km. The cross-path horizontal wind moves the scatterers and variations in C_n^2 through the common volume and, with an assumed 10 m/s cross-path velocity, replaces the scatterers in the common volume in about 30 seconds. The 30 or 120 second averaging removes the higher frequency fluctuations produced by three-dimensional turbulence in the inertial subrange.

The larger scale $k^{-5/3}$ spatial spectrum produces an $f^{-5/3}$ spectral region which should be evident at frequencies below about 10^{-4} - 10^{-3} Hz depending on the cross-path wind velocity. For two-dimensional turbulence the spectrum should decrease as f^{-3} at frequencies greater than the high frequency limit to the $f^{-5/3}$ region. The expected f^{-3} behavior is evident in the spectra in Figure 5 for both radio frequencies as illustrated by the dot-dashed curve. At the larger spatial scales and longer averaging times represented by the data in the figure, the field strength at both frequencies is proportional to C_n^2 averaged over the scattering volume. The resulting spectra for the two radio frequencies are therefore identical when the logarithm of the received signal is used for analysis. Because the linear signal level fluctuations have been normalized by the median signal level, the spectra are also the same for the linear signals. The f^{-3} spectral shape has also been observed in weather radar observations of rain and is expected for bistatic scattering or troposcatter under rainy conditions. The f^{-1} region evident at even higher frequencies is also present in

weather radar observations of rain. The data in Figure 5 do not show a $f^{5/3}$ region presumably because the cross-path wind velocity is too small.

Clear weather observations

Data were recorded in eleven observation sets on nine separate days during the measurement campaign. Five of the sets were for clear weather conditions and the remainder were for light to moderate rain conditions somewhere on the path. Short measurement runs were made at other times, primarily while the equipment and computer programs were being debugged, but time series long enough for statistical analysis were not recorded. Initially, the horn antennas were used during the receive antenna alignment exercises. Short data runs were made with the horn antennas during clear weather conditions for comparison with interleaved measurements with the dish antennas used for the longer data runs. In agreement with the predictions of turbulent volume scattering models, the relative received signal levels averaged over periods of ten minutes or more differed by the ratio of the receiver antenna gains in the direction of the radio horizon on the great circle path between the transmitter and receiver. These results were obtained consistently at both frequencies.

Figures 2 through 5 display results for one of the five measurement sets for clear weather conditions. For four of the five sets, the Rayleigh fading typical of the short-term fluctuations in signal level was reduced to less than 3 dB peak-to-peak with 30 seconds of averaging. For the fifth set, the peak-to-peak values after 30 seconds of observation were still over 20 dB at C-band indicating that the averaging interval was too short for the fluctuation rate at that frequency. The Ku-band signals also reached more than 15 dB above the clear weather median level calculated from data from the four other data sets. This set was not used in the statistical analysis of clear air conditions but is described in the subsection below on enhanced signals.

The cumulative received signal level distributions for the two frequencies for averaging intervals long enough to extract the underlying lognormal nature of the median or average variations in signal strength (120 sec) are displayed in Figure 6. The observed median received signal level for Ku-band was -112 dBm and was -98 dBm at C-band. The C-band median level estimated from the straight line, lognormal fit to the data was -99 dBm and the Ku-band median level estimated in the same way was -112 dBm. The values from the lognormal model fits were used to estimate the median levels for comparison with model predictions because the model fit has less statistical error. The standard deviation listed in

the figure is from the slope of the lines fit to the cumulative distributions. It is the same at both frequencies. The median transmission loss values corresponding to the median level estimates, 144 dBm and 157 dBm for C-band and Ku-band respectively, were used for comparison with the different model predictions of transmission loss for troposcatter communication links. Table 2 displays predictions for the Prospect Hill to Mt Tug paths by the three models recommended by the CCIR [1986; 1988]. All three models were corrected to include the increase in loss due to gaseous absorption and the difference between the maximum antenna gain and the gain toward the radio horizon. Although these correction are not included in the referenced reports of the CCIR, they are included or implied in their documents addressing interference prediction. Table 3 presents predictions made using the bistatic radar equation and the scattering cross section per unit volume for the fluctuations in the refractive index of the atmosphere produced by three-dimensional turbulence within the common volume of the transmit and receive antenna patterns [Crane, 1973]. The volume scattering model was extended to predict the received power vs delay profile and delay spread for the Ku-band link.

The standard model for the prediction of transmission loss, CCIR model I based on the earlier work of Rice et al [1965], is designed to forecast the annual distribution of hourly median values. For a particular link, the standard deviation of the prediction error of the median value of the hourly median values is estimated to be 4 dB. At Ku-band the prediction error is 1 dB and at C-band the prediction error is 3 dB, within the expected prediction uncertainty for a year of data and well within any expected error bounds for only 12 hours of observations. If the model were valid at both frequencies, the prediction errors would not differ by 2 dB but be the same for both frequencies. Even with a short run of data, models can be tested as long as the data are for the phenomena to be forecast. A problem with the CCIR standard model is that it does not attempt to distinguish between the several different propagation phenomena that contribute to the received field strength statistics. Because the dominant propagation mode for a typical tropospheric scatter path is turbulent volume scatter or thin layer scatter depending on the frequency, it is not surprising that the model predictions are as close to the measurements as they are.

The bistatic turbulent volume scatter model provides a better prediction for both the absolute median received signal levels and the relative difference between the median levels at the two frequencies. The model is a refinement of the procedure described by Crane [1973; 1981] to include power level vs delay profiles. The input necessary for the use of the bistatic scattering model is the structure constant, C_n^2 , for the turbulent fluctuations in

refractive index. For the Prospect Hill, Mt Tug path, the average of the C_n^2 profiles made for the same geographical area using the L-band radar at Millstone Hill [Crane, 1981] as reported by Gossard [1977] was used in the calculations. The radar measurements were for a limited number of days but were selected to represent only clear air conditions. The resulting agreement between model predictions and measurements is very good. The prediction for the median of the C-band signal levels is low by 1 dB as is the prediction for Ku-band. The relative difference is within 1 dB of the observed difference between the two frequencies. Simultaneous measurements of radar backscatter at L-band and clear air troposcatter at X-band for a variety of scattering angles showed that tropospheric scattering at frequencies of X-band and above should be modeled as caused by turbulent volume scattering [Crane, 1973]. The current results support the earlier finding.

The other models described in the reports of the CCIR, method II and a model suggested by the Chinese to replace method I, are the same as method I for the prediction of the relative signal levels at the two frequencies. The models produce identical results because the frequency dependent factors are the same. Again, the models were adjusted to include attenuation by atmospheric gasses and directive gain towards the horizon. The performance of the other CCIR models is different from method I in the prediction of the absolute transmission loss values, method II is without error at C-band and within 2 dB at Ku-band. The predictions of the proposed replacement for method I differ from the observations by 5 dB at C-band and 7 dB at Ku-band. CCIR method II is an independent fit to many of the same experimental results employed by Rice et al. [1965] in the development of the predecessor to method I and seems to perform better than method I (on the basis of a very limited data set).

The clear weather observations were made during the first half of the measurement campaign while the computer processing for advancing and retarding the PRN code (changing lags) was still being debugged. As a consequence, the carrier only, carrier plus twelve lag sampling schemes were in use for data recording but consistent tracking of the lag with the maximum signal did not occur. The data from the correlation detectors could not be used to estimate the delay spread for the clear weather measurements.

Days with Rain

The short time duration observations made prior to the measurement campaign generally showed a marked increase in the signal level during rain over the values forecast for the clear atmosphere. The highest signal levels recorded during the measurement

campaign are displayed in Figure 7 as are the lowest. These data show increases in the Ku-band signal relative to the clear weather Ku-band median level of over 25 dB and increases relative to simultaneous observations at C-band that exceed 30 dB after adjustment for differences in the long term clear weather median values. The lowest signal levels were also observed during the observation period but, the C-band signals were also at low values at the same time. For this data set, the Ku-band signal was not modulated and no delay data were recorded. The carrier signal level is 12 dB higher than when modulated. The received power level values were adjusted to match the values that would have been received if the carrier were modulated. The carrier detection and correlation detection channels have a rather narrow dynamic range, less than 20 dB. Computer controlled switching attenuators were used to keep the received signal within the center of the dynamic range of the receiver system. The Ku-band signal levels reached more than 70 dB above the receiver noise level.

The C-band signal level was consistently 10 dB or more below the clear weather median level with the exception of a few 15 minute intervals when the levels at both Ku-band and C-band increased together. These intervals correspond to the passage of rain cells through the scattering volume. The rain cell structure evident at Ku-band is also present in the C-band data but at a reduced magnitude. The scattering cross section per unit volume of rain varies as l^4 while for refractive index fluctuations the wavelength dependence of the scattering cross section per unit volume is $l^{-1/3}$. The increase in scattered signal at Ku-band relative to C-band is countered by attenuation due to rain which is larger at the higher frequency. The rain scatter is barely detectable above the clear air turbulent volume scattering at C-band but is obvious at Ku-band. Of as much interest for troposcatter communications is the depression in the C-band clear air turbulent volume scattered signal levels observed during the periods between rain showers. The depressed signal levels also occurred at Ku-band and are more likely the cause of the lowest Ku-band signal levels observed during the experiment than is increased attenuation by rain on the path.

The curves for the two radio frequencies plotted in Figure 7 should coincide if clear weather turbulent volume scattering is the propagation mode responsible for signal transmission. Coincidence is evident only during a period of less than an hour between 1 and 2 am. During the remainder of the measurement period, rain scatter is evident at Ku-band. Figure 8 presents the same observations as Figure 7 but with the C-band data re-scaled to represent predictions of the Ku-band signal for rain scatter without attenuation.

The bistatic radar equation and the l^{-4} behavior of the scattering cross section per unit volume of rain were used in the frequency scaling. The C-band signals were increased by 19 dB for display in the figure to adjust both for rain scatter and the differences in median signal levels for clear weather turbulent volume scattering. The rain scatter predictions at Ku-band and the Ku-band observations reach nearly the same magnitude in rain cells in the scattering volume up through about 5 am. Apparent time shifts exist between the curves due to the different size and shifted location of the center of one scattering volume relative to the other (see Figure 1). After 5 am, the Ku-band signal exceeded the predictions from the C-band measurements by about 10 dB. The times when the Ku-band measurements are well below the predictions based on the occurrence of rain correspond to intervals when scattering via clear air turbulence exceeds scattering by rain at C-band.

Working back through the bistatic radar equation at C-band, the peak reflectivity value corresponding to the rain cell in the scattering volume at 4.6 am. is 27 dBZ if the 44 km long scattering volume is filled uniformly. Assuming the Marshall-Palmer relationship between reflectivity and rain rate, the rain rate in the scattering volume was 1.8 mm/h. If the rain cell were only 2 km across, the reflectivity in the cell would be 40 dBZ which corresponds to a 12 mm/h rain rate. For a 1.8 mm/h rain spread uniformly over the entire troposcatter path, the attenuation at 5 GHz would be 0.4 dB and the attenuation at 16 GHz would be 14 dB. A comparison between the 16 GHz observations and the predictions scaled from 5 GHz shows little in the way of attenuation except perhaps at about 3 am. when attenuation values of about 5 dB may have occurred. The two hour period after 5 am. is characterized by Ku-band signal levels 5 to 10 dB higher than expected for the C-band data using the equations for rain scatter. The maximum increase for rain cells which span only a small fraction of the scattering volume at Ku-band is less than 1.4 dB. The observed increases may be due to enhanced forward scattering by melting ice (bright band) within the scattering volume.

The power spectra for signal level fluctuations (in dB) are presented in Figure 9 for the data in Figure 7. The Ku-band spectra closely follow the $f^{-5/3}$, f^{-3} , and f^{-1} segmented power law structure described above for two-dimensional turbulence. In this case, a $f^{-5/3}$ region is evident at a frequency corresponding to a cross-path wind velocity of the order of 5 m/s. These spectra have the same shape as the spectra calculated from weather radar maps of the logarithm of reflectivity or of the logarithm of rain rate [Crane, 1987]. The weather radar observations provided two-dimensional spatial series and the one-dimensional spatial spectra were obtained by azimuthally averaging the two-dimensional

spectra. The equivalence of the two spectra, time and space, are a consequence of Taylor's hypothesis. The weather radar observations have shown that the shape of the spatial spectrum is universally observed for rain in different climate regions and different storm types. The shape of the temporal spectrum at C-band is similar to the shape of the spectrum at Ku-band but the signal level variance represented by the spectra is higher at Ku-band than at C-band because a large fraction of the time with rain corresponded to periods with turbulent volume scattering at C-band masking scattering by rain.

The estimated cross-path velocity and the time duration of the signal level peaks in Figure 8 can be combined to provide an estimate of the rain cell size and, from the fractional scattering volume filling, the peak reflectivity in a cell. For the cell at 4.6 am., the time duration at half reflectivity level (-3 dB signal level) was 11.4 minutes which corresponds to a cross-path cell size of 3.4 km. Assuming an azimuthally symmetric cell, only 8 percent of the scattering volume was filled. The peak reflectivity in the cell was therefore 38 dBZ. The peak rain rate was 8.8 mm/h and the maximum attenuation produced by the cell was 1.5 dB. At the higher frequency, forward scattering is increased slightly relative to the forward scattering at C-band so the net difference between the Ku-band predictions from the C-band measurements and the Ku-band signal levels would be 1.3 dB [Crane, 1974]. The difference in fractional volume filling between the two frequencies produces a 1.4 dB increase in the Ku-band signal level relative to the C-band signal which nearly compensates for the net decrease due to forward scattering differences and attenuation. From Figure 8, the Ku-band signal level measurements at the cell peak and the Ku-band predictions from the simultaneous C-band measurements agree almost exactly.

Results similar to those for April 6 and 7, 1987 were obtained for each of the other days with rain. The data in Figure 7 represent the largest swings in received signal level observed in the experiment but signal level increases above the clear weather median level by more than 10 dB were common. C-band signal level depressions of more than 10 dB relative to the clear weather median level were also common. These data are best summarized by the cumulative distributions of signal level on days with rain. Figure 10 displays the distribution functions for 120 second averages and includes, for reference, the lower signal extremes of the clear weather distribution from Figure 6. These data show nearly identical median values for both Ku-band and C-band. The signal levels seem to approach the clear weather conditions for a reduced variate above 2 (1 percent of the time

with rain). The C-band data clearly show the depression in signal level near the median value (reduced variate = 0).

The experiments in rain were generally run after the program to track the lag with the maximum signal was debugged. Delay spread observations were available for all but the April data. Examples of the average delay profiles for two days with intermittent light rain, August 26 and 27, 1987, are presented in Figure 11. Delay spread was estimated from the profile measurements by calculating the standard deviation of the received power weighted tap numbers times $2\sqrt{2}$ times the delay per tap. This estimate works well when the signal to noise level is high. In the absence of a signal, the variance is very wide. To make the estimation system more robust, only data from taps 1 through 6 were used in estimating the delay spread. The results for the average delay profiles in Figure 11 are 115 nsec for August 26 and 131 nsec for August 27. The bistatic scatter model estimates are 12 nsec for turbulent volume scattering and 16 nsec for rain scatter (Table 3). These very narrow delay spreads (channel impulse responses) must be convolved with the PRN code and then correlated with the code to provide the model estimate for turbulent volume scatter plotted in the figure. The observed spread values are inflated by the poor resolution caused by a relatively low code bit rate. The modeled spread value is inflated from 12 to 105 nsec by the poor resolution. The differences between the model prediction curves for rain and turbulent volume scatter are too small to resolve in the figure. The averages for the two data sets are coincident with the model profile as shown in Figure 11.

The delay spread time series for September 18, 1987 is presented in Figure 12 along with the time series for signal level relative to the clear weather medians. For this day, the depression in the C-band signal level was not evident. The enhanced signal levels at Ku-band were present throughout the entire observation period. The delay spreads had values close to the averages displayed for the two days in August. The delay spread tended to increase with decreasing signal level but the change was small and could be primarily a result of the decrease in signal to noise at the correlator output. No significant increases in delay spread were observed for any of the days with rain.

Enhanced signals

Data from one of the clear weather periods still showed excessive variations in signal level at C-band after 30 seconds of integration. The time series of 120 second averages are displayed in Figure 13. The data are for the afternoon of August 26, 1987 seven hours before the data set with rain used to prepare the average delay spread profile in Figure 11.

Enhanced signal levels are present at 16 GHz but the signal levels are depressed by as much as 15 dB at 5 GHz for long time intervals. The delay spreads for this time period are among the smallest observed during the measurement campaign.

The power spectra for this data set are displayed in Figure 14. In this case, the variance at C-band is greater than at Ku-band, the reverse of the results for enhanced signals at Ku-band in rain. The shape of the spectra are also significantly different from the turbulent scatter or rain cases. For this data set, the f^{-1} region is the only region evident in the spectrum. This spectral shape could result from a significantly reduced cross-path wind velocity but the increased variance at C-band would not be expected under such conditions. A possible explanation is coupling into an elevated layer where the coupling constant at C-band is smaller than at Ku-band or the propagation constant for the trapped waves in the layer implies significantly more attenuation at C-band than at Ku-band.

5. CONCLUSIONS

The results of the first measurement campaign are 1) troposcatter may be used for reliable communication at Ku-band, 2) the observed delay spread values are marginally larger than the minimum resolvable value for the pseudorandom code rate used in this experiment, 3) enhanced signal levels were evident in rain with little increase in delay spread, 4) depressed signal levels were obtained in rain at C-band when turbulent volume scattering dominated rain scatter at that frequency, 5) excessive rain attenuation events were not observed but high rain rates were not encountered during the measurement campaign, 6) enhanced signal levels not associated with rain were encountered at Ku-band and 7) the delay spread values for the enhanced signal conditions were among the smallest recorded. Three propagation modes were in evidence for this path, turbulent volume scattering (the normal troposcatter mode), rain scatter and enhanced signal levels not associated with rain. The latter effect may be due to coupling via elevated layers. A finer resolution channel probe is needed to explore the delay spread that actually occurs on the path.

ACKNOWLEDGEMENTS

The experiment described in this paper was sponsored by the Rome Air Development Center (RADC). The work at the Thayer School of Engineering, Dartmouth College was

supported by RADC through their Post-Doctoral Program. The receiver site on Mt. Tug is the cable head facility for Twin State Cable of West Lebanon, NH. The generosity of Twin State Cable in allowing us to use the facility is appreciated. The sufferance of the cable company is gratefully acknowledged particularly on days when the Ku-band receiver interfered with several of the TV channels. A number of graduate students at the Thayer School of Engineering were involved in the project. Particular thanks go to Chet Levins, Mike Sullivan and Peter Stamboulis for their many hours in working on the receiver equipment and recording the data.

REFERENCES

- Abel, N [1972]; Beobachtungen an einer 210 km langen 12 GHz Strecke (Observations on a 12 GHz link of 210 km length), A455 TBR34, Techn. Ber. FTZ, Darmstadt, FRG
- CCIR [1986]; Propagation data and prediction methods required for trans-horizon radio-relay systems, Rept 238-5, Recommendations and Reports of the CCIR, Vol 5, Propagation in Non-Ionized Media, ITU, Geneva.
- CCIR [1988]; Propagation data and prediction methods required for trans-horizon radio-relay systems, Draft Rept 238-5(MOD I), Conclusions of the Interim Meeting of Study Group 5 (Propagation in Non-Ionized Media), ITU, Geneva.
- Crane, R. K. [1973]; Analysis of data from the Avon-to-Westford experiment, Tech. Rept. 498, MIT Lincoln Lab., Lexington, MA.
- Crane, R. K. [1974]; Bistatic scatter from rain, *IEEE Trans Antennas and Propagat.*, AP-22(2), 312-320.
- Crane, R. K. [1980]; A review of radar observations in the lower stratosphere, *Radio Sci.*, 15(2), 177-193.
- Crane, R. K. [1981]; A review of transhorizon propagation phenomena, *Radio Sci.*, 16(5), 649-669.
- Crane, R. K. [1987]; Space-time structure of precipitation, Preprints 10th Conf. Probability and Statistics in Atmospheric Sciences, Amer. Meteorol. Soc, Boston, MA. 265-268.
- Gossard, E. E. [1977]; Refractive index variance and its height distribution in different air masses, *Radio Sci.*, 12(1), 89-105.
- Levins, C. L. [1986]; Establishing a receiver station for the study of a Ku band troposcatter channel, Master of Engineering Thesis, Thayer School of Engineering, Dartmouth College, Hanover, NH.
- Olsen, R. L. and U. H. W. Lammers [1978]; Bistatic radar measurements of ice-cloud reflectivities in the upper troposphere, *Electron. Letts.*, 14(7), 219-221.

- Rice, P. L., A. G. Longley, K. A. Norton and A. P. Barsis [1965]; Transmission loss predictions for tropospheric communication circuits, Vol. I and II, NBS Tech. Note 101, U. S. Dept. of Commerce, Washington, D. C.
- Stamboulis, P. [1987]; The study of a tropospheric scatter channel via system modeling and analysis of data collected from Ku and C band links, Master of Science Thesis, Thayer School of Engineering, Dartmouth College, Hanover, NH.
- Sullivan, M. J. [1987]; The establishment of a dual frequency troposcatter receiver station for use in a statistical study of the feasibility of troposcatter in the Ku band, Master of Engineering Thesis, Thayer School of Engineering, Dartmouth College, Hanover, NH.
- Tatarski, V. I. [1961]; *Wave Propagation in a Turbulent Medium*, McGraw-Hill Book Co., NY.
- Vilar, E., C Spillard, M. Rooryck, M. Juy, P. C. Barber and M. P. M. Hall [1988]; Observations of troposcatter and anomalous propagation signal levels at 11.6 GHz on 155 km path over the sea, *Electron. Letts.*, **24(10)**, 1205-1206.

Table 1

Troposcatter Path Characteristics

Variable	Units	Link Values	Path 1	Path 2
Frequency	GHz		4.95	15.73
Wavelength	cm		6.06	1.91
Trans. Location				
Latitude	deg	42.3886		
Longitude	deg	71.2544		
Rec. Location				
Latitude	deg	43.6639		
Longitude	deg	72.1847		
Central Angle	mrad	25.22		
Surface Distance	km	160.9		
Trans. Height	m	159.4		
Rec. Height	m	493.8		
Horizon Angle Trans.	deg	-0.05		
Horizon Angle Rec.	deg		0.23	0.23
Transmit Aperture	ft	29 00		
Transmit Beamwidth	mrad		8.36	2.63
Receive Aperture	ft		10	3
Receive Beamwidth	mrad		25.25	26.49
Scattering Angle	mrad		34.61	35.23
Specific Attenuation:				
Oxygen	dB/km		0.0062	0.0085
Water vapor	dB/km		0.0014	0.0256
Transmitter Power:				
Unmodulated	watts		30	500
Modulated				30
Receiver Noise Level	dBm		-146	-144

Table 2

Thin Layer Troposcatter Model Predictions

CCIR Calculations [CCIR,1986]

Variable	Units	Link Values	Path 1	Path 2
Method I				
30 log (f)	dB		111	126
-20 log (d)	dB	-44.13		
theta*d	km		3.54	3.54
F(theta*d); Ns = 350	dB		150	150
G trans.	dB		50	60
G rec.	dB		41	41
Coupling loss	dB		11	17
d1	m	142.87		
dse	km		18	12
de	km		130	136
v(de) Type 6	dB		2	2
gaseous absorption	dB		1	5
Line Losses	dB		2	2
L(50) median	dB		138	153
Adjust for G rec. at Horizon	dB			3
Corrected L(50)	dB		141	156
Difference(50)	dB			15
P rec median	dBm		-96	-111
St. Dev L(50)	dB		3.6	3.6
L(99)	dB		155	171
P rec 99%	dBm		-110	-126
L(1)	dB		120	135
P rec 1%	dBm		-75	-90
Method II				
Equivalent distance	km		187	187
L(50,1 GHz) Temp. Cl.	dB		201	201
20 log (d/dq)	dB		-2	-2
Lc - Gt - Gr - 3	dB		-83	-87
30 log (f), f in GHz	dB		21	36
gaseous absorption	dB		1	5
L(50) median	dB		144	159
Difference(50)	dB			15
P rec median	dBm		-99	-114
Chinese Rev. Method I [CCIR,1988]				
M Climate 6	dB	30		
30 log (f)	dB		111	126
10 log d	dB	22		
30 log (scat.angle)	dB		46	46
gamma Climate 6	km ⁻¹	0.27		
N(H,h)	dB		16	16
Lc - Gt - Gr - 3	dB		-83	-87
gaseous absorption	dB		1	5
L(50) median	dB		149	164
Difference(50)	dB			15

P rec median

dBm

-104

-119

Table 3

TRANSMISSION LOSS and RECEIVED POWER LEVEL PREDICTIONS
using the BISTATIC RADAR EQUATION

Path length: 160.9
 Ku-band at F = 15.73 GHz, C-band at F = 4.95 GHz
 Transmitter half power beamwidths Ku, C (deg): 0.15 0.48
 Receiver half power beamwidths Ku, C (deg): 1.52 1.45
 Elevation angle for transmit antenna (deg): -0.05
 Elevation angle at receiver Ku & C (deg): 0.98 0.95
 Absolute delay = 536.3 microsec.

Tap	Height km	Range Trans km	Range Rec. km	Elev Rec. deg	Received Power mwatt	S/N	Scatter Angle mrad	C_n^2 m ^{-2/3}
0.00	0.82	113.2	47.7	0.23				
1.00	1.28	145.4	15.5	2.84	4.5e-12	30.7	31.62	9.5e-16
2.00	1.38	151.7	9.3	5.46	5.0e-16	-8.9	82.68	7.8e-16
3.00	1.43	154.3	6.6	8.06	6.9e-26	-107.5	130.09	7.5e-16

Turbulent volume scatter, scattering volume filled
 Power Ku: -113.4 dBm, Power C: -100.4 dBm
 T_Loss Ku: 158.2 dB, T_Loss C: 145.2 dB, Diff: 13.0 dB
 Delay Spread Ku: 12.1 nsec

Rain scatter without attenuation for 10 mm/h rain rate, scattering volume filled uniformly
 Power Ku: -76.8 dBm, Power C: -82.4 dBm
 T_Loss Ku: 121.6 dB, T_Loss C: 127.2 dB, Diff: -5.6 dB
 Delay Spread Ku: 16.3 nsec

APPENDIX B

Data Set	Date	Identifier	Weather Conditions	Median Levels		Delay Spread (nsec)
				Ku (dBm)	C (dBm)	
1	April 6, 7 1987	OVNT47	Rain	-108	-110	No
2	June 5, 1987	STD65	Clear*	-110	-93	No ¹
3	June 16, 1987	STD616	Clear*	-122	-108	No ¹
4	July 30, 1987	STD730	Clear*	-117	-101	No ¹
5	August 3, 1987	STD83	Clear*	-107	-99	No ¹
6	August 10, 1987	STD810	Rain	-116	-112	No ¹
7	August 26, 1987	STD1_826	Clear**	-102	-114	108
8	August 26, 1987	STD2_826	Rain	-115	-110	180
9	August 27, 1987	STD1_827	Rain	-105	-100	128
10	August 27, 1987	STD2_827	Rain	-105	-99	96
11	September 18, 1987	STD918	Rain	-99	-97	128
*Clear			-112	-98		
Rain			-108	-107		
**Enhanced			-102	-114		

¹ Program to track the lag with the maximum signal level not working.

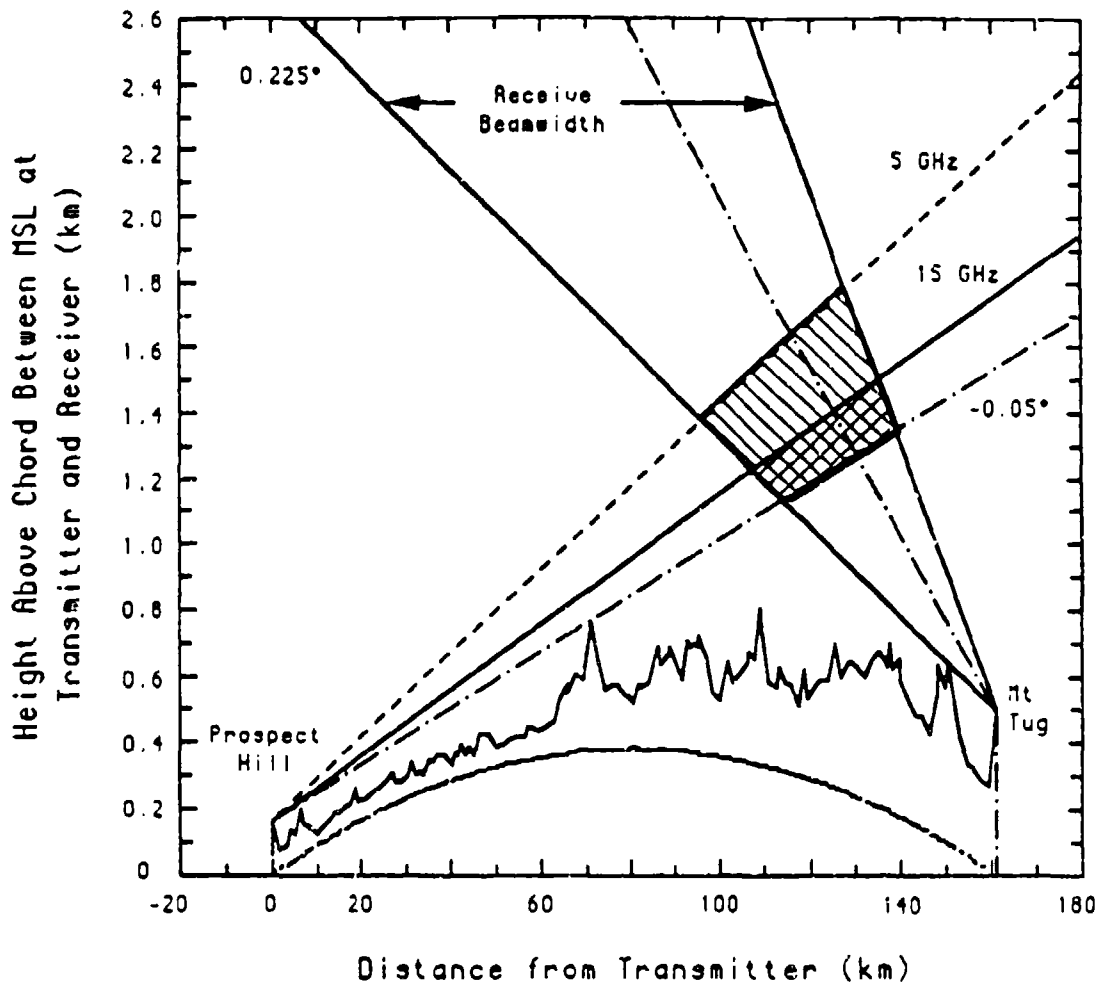


Figure 1 Troposcatter Path Profile over a 4/3 Effective Earth Radius. The scattering volumes are cross hatched. The transmit antenna is pointed at the horizon and only the portion of the beam above the horizon is displayed.

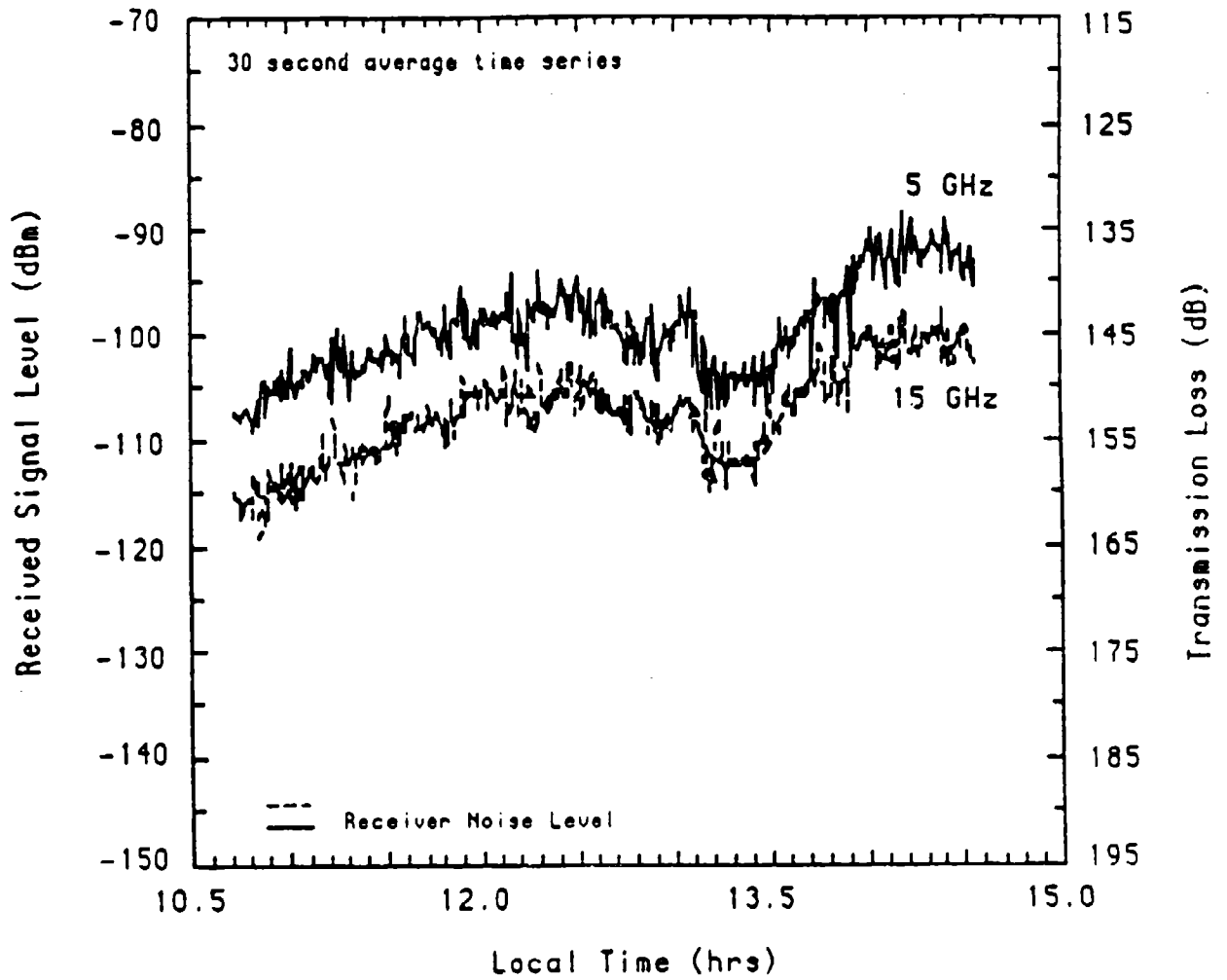


Figure 2 Received signal levels for 30 watt transmitter power. Data are for clear weather conditions on August 3, 1987.

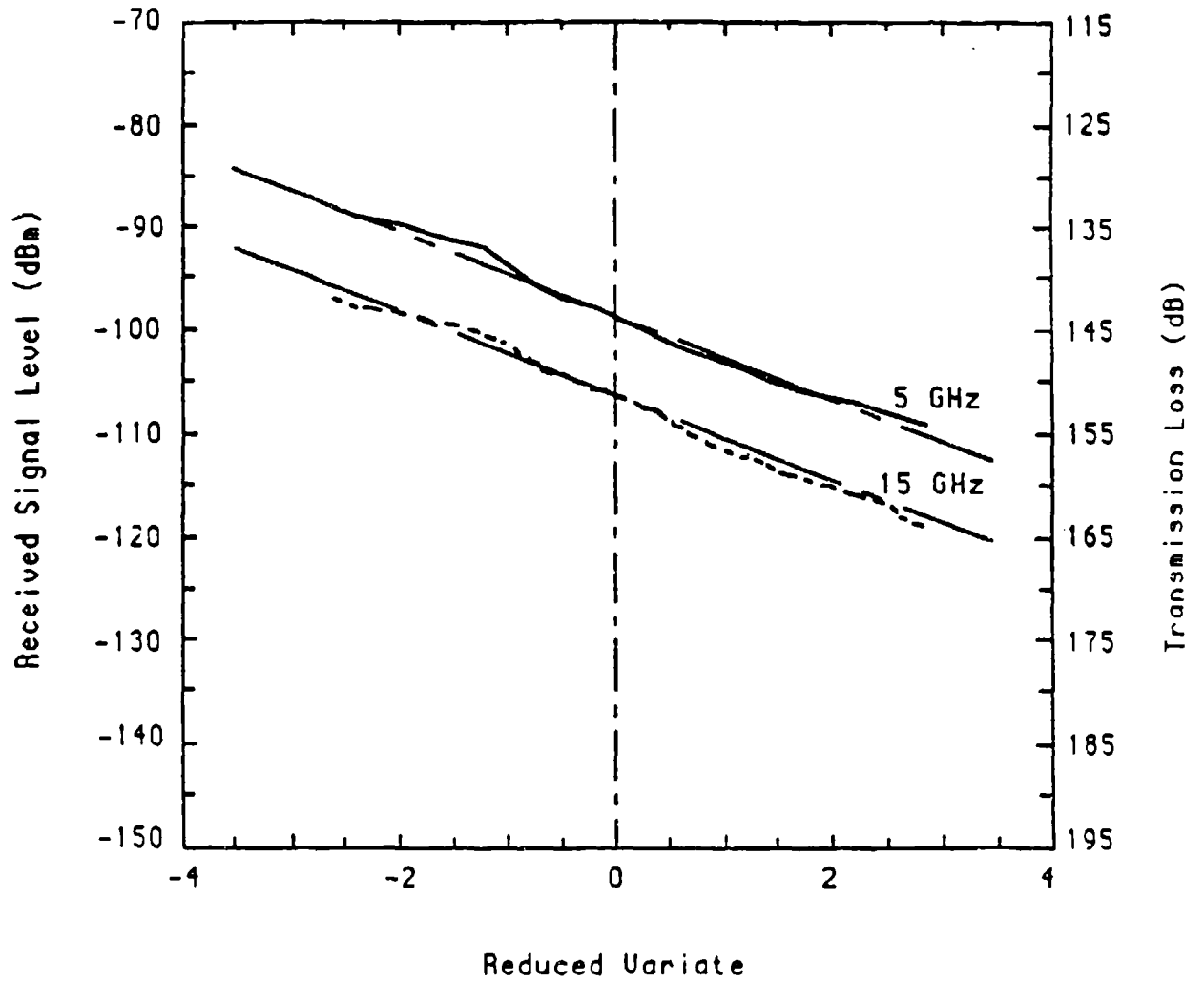


Figure 3 Cumulative signal level distributions for the data in Figure 2.

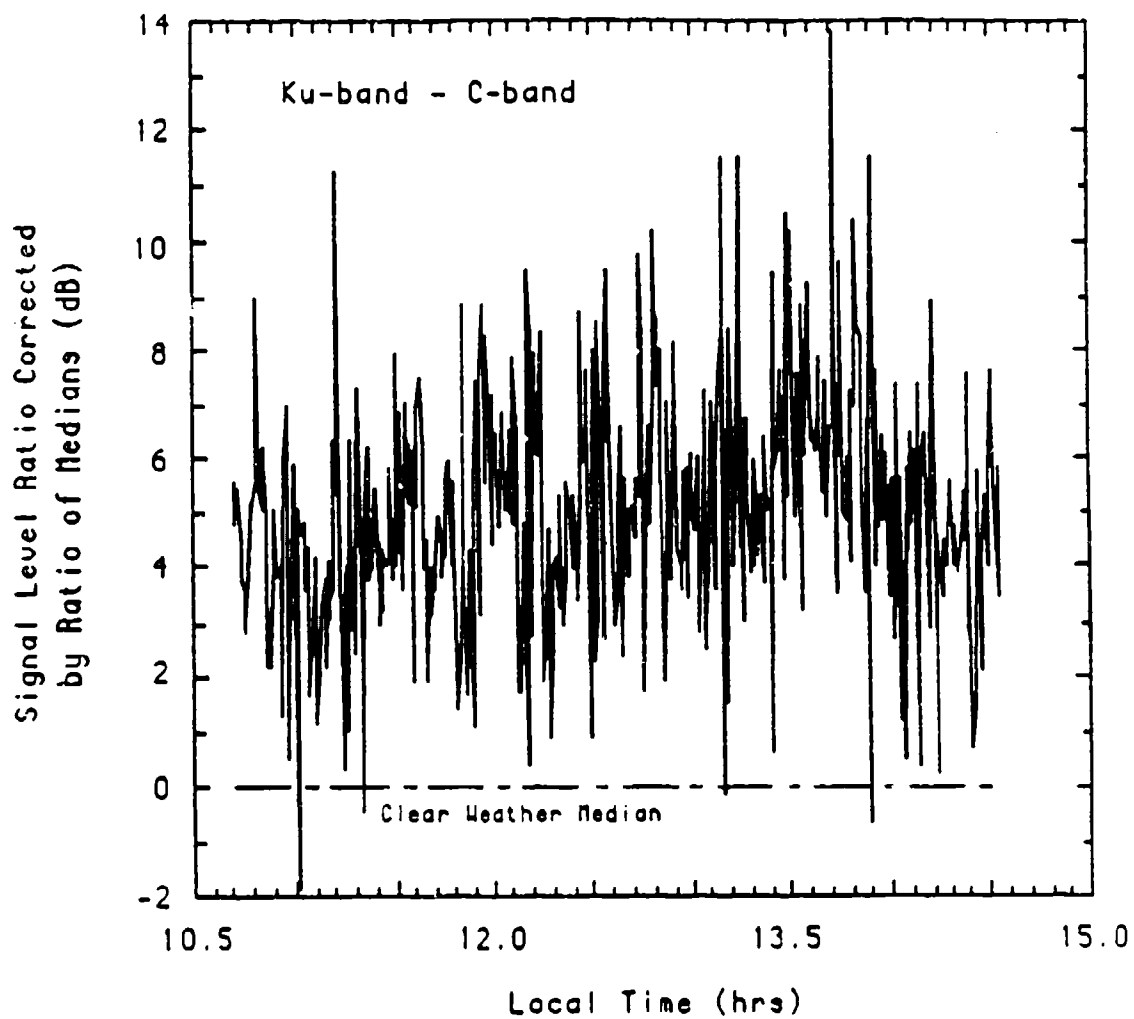


Figure 4 Ratio of Ku-band to C-band signal levels normalized by the ratio of the C-band to Ku-band median values. Data are from Figure 2.

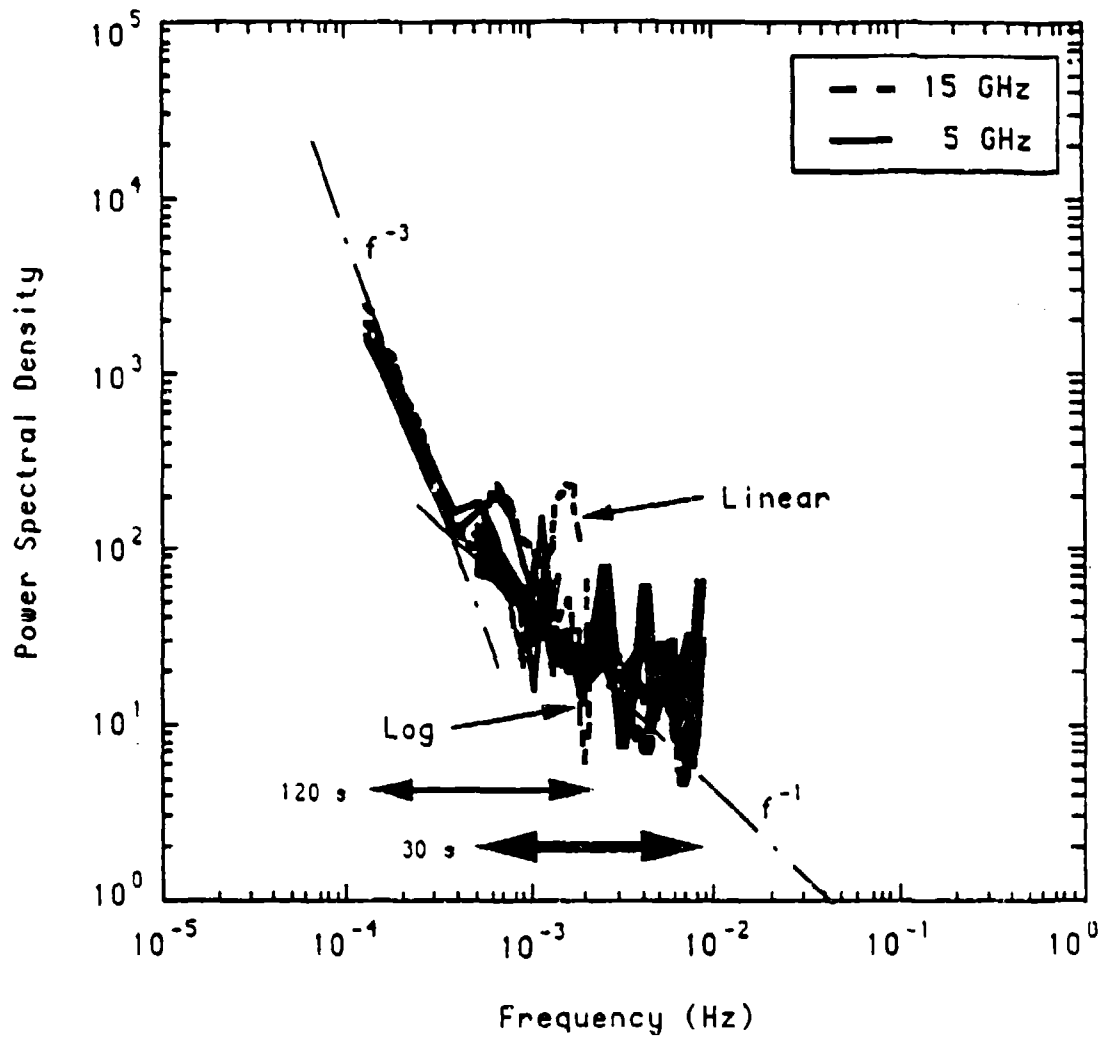


Figure 5 Power spectra for signal level fluctuations at 5 and 15 GHz. A total of eight spectra are plotted, half for the signal level and half for the logarithm of the signal level. Data are from Figure 2.

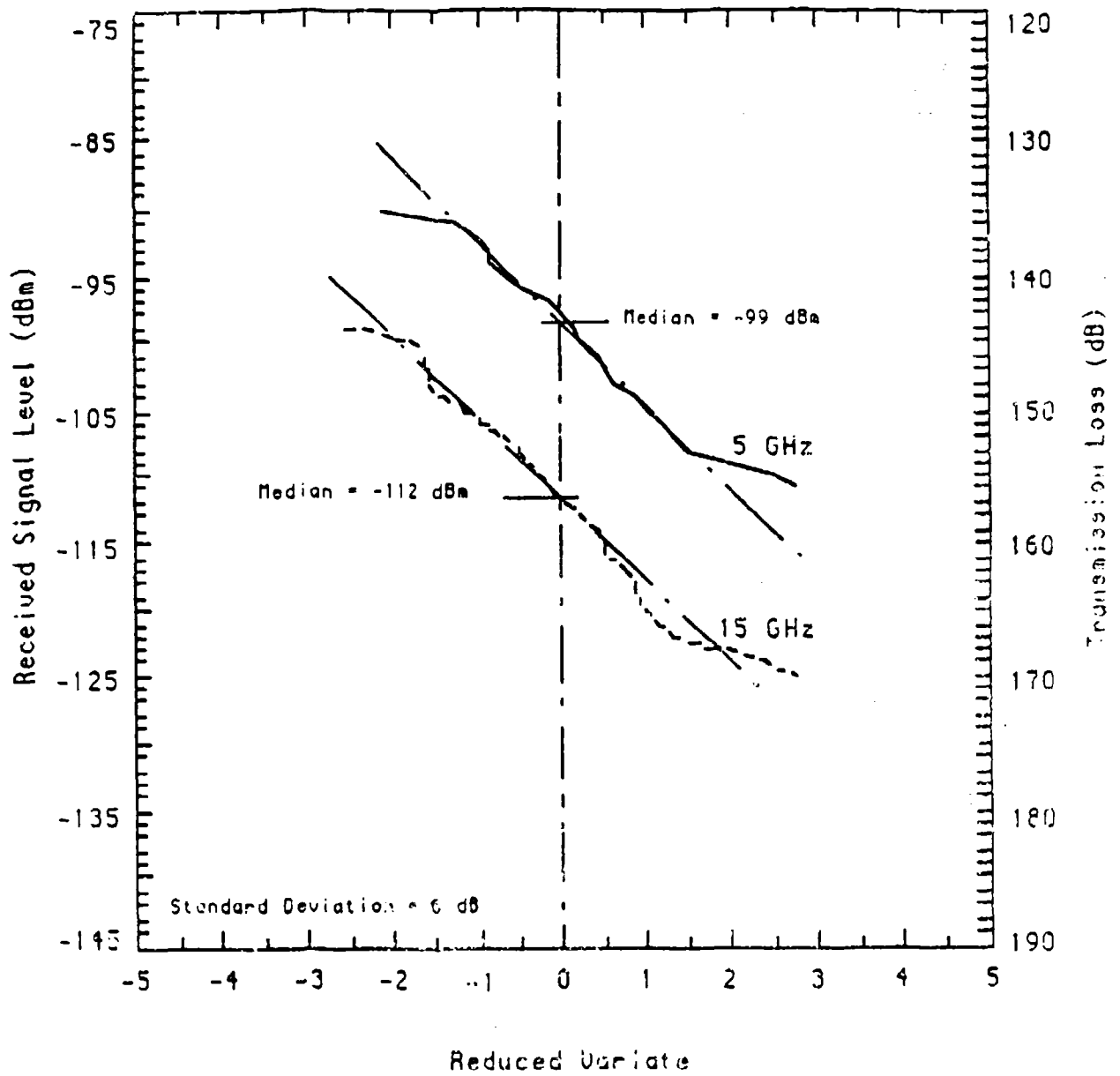


Figure 6 Cumulative signal level distribution for clear weather conditions

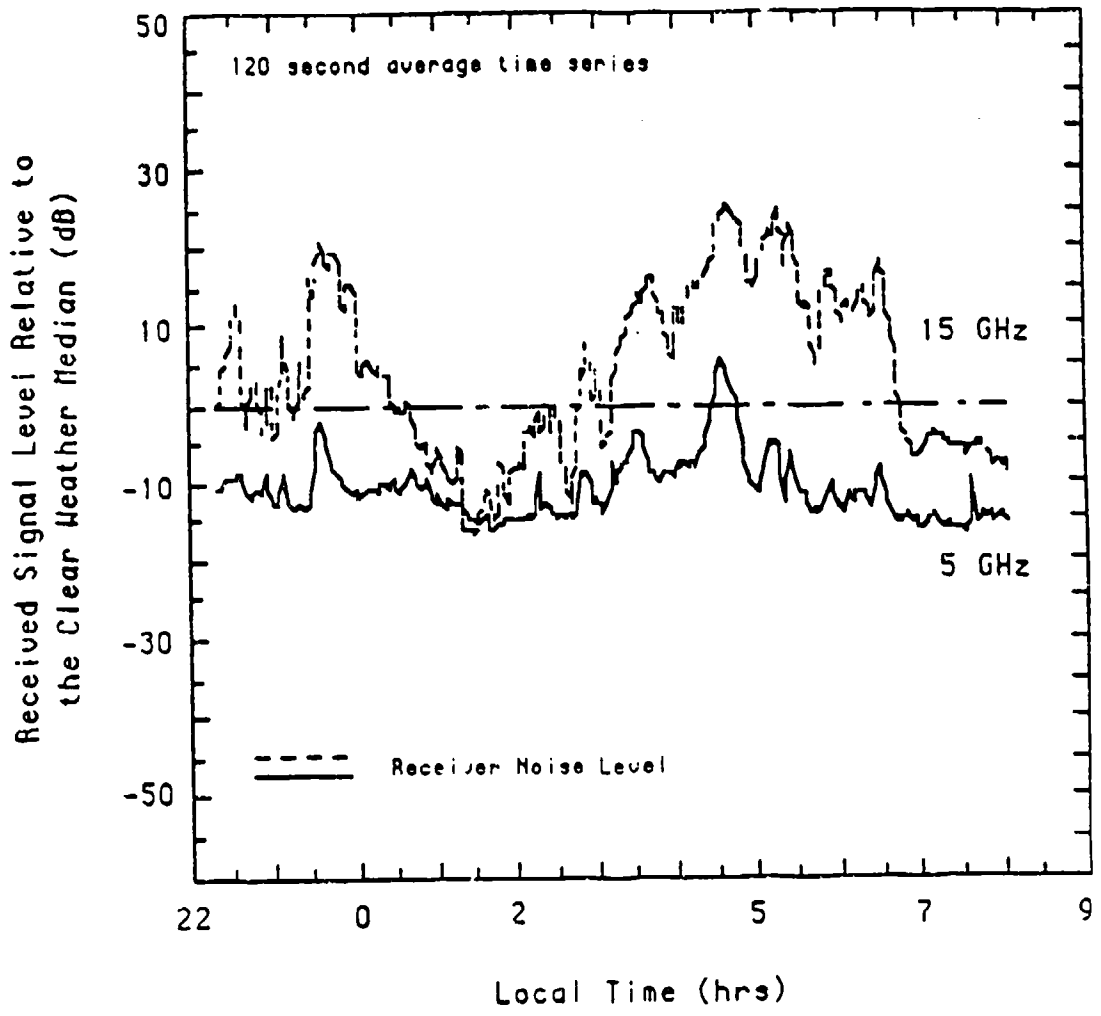


Figure 7 Received signal levels relative to the clear weather median levels for rain during the night of April 6 - 7, 1987.

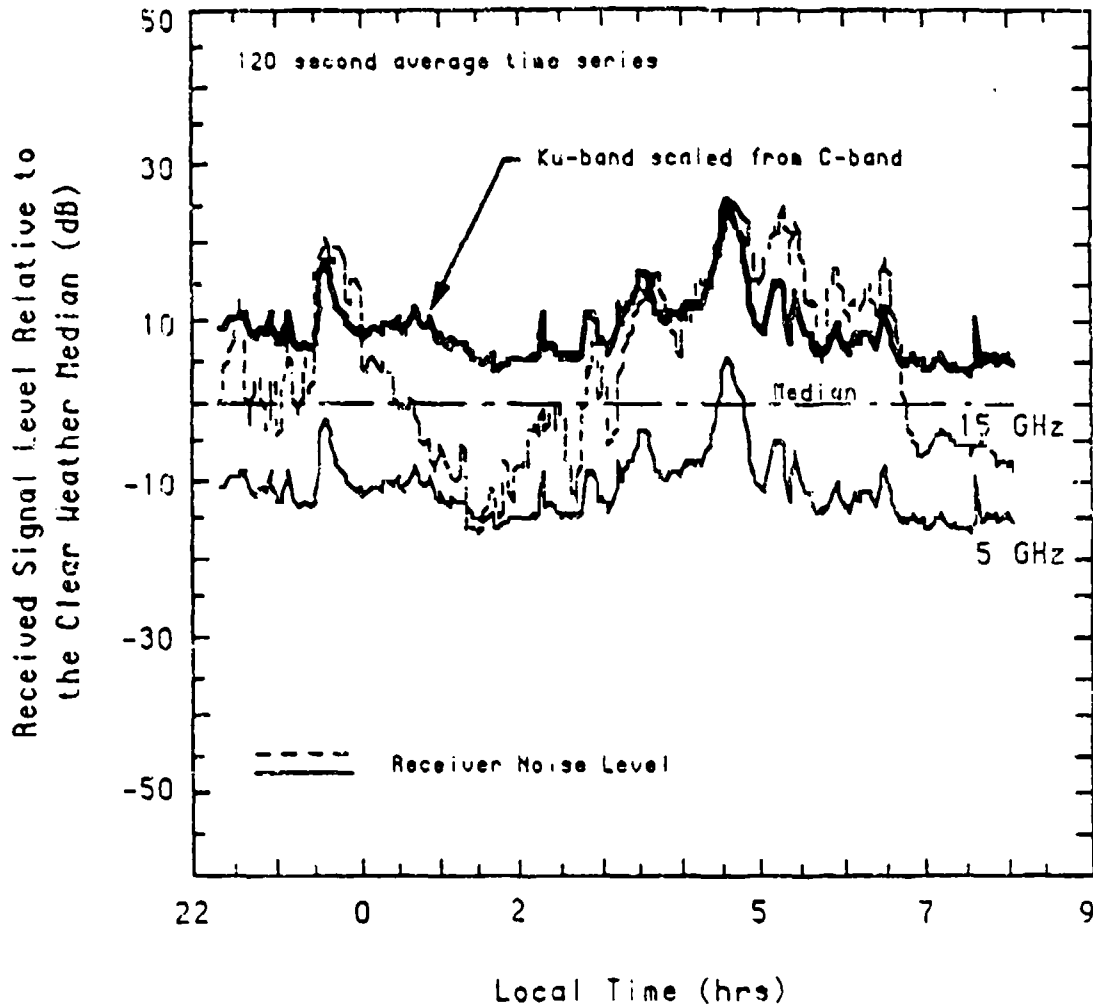


Figure 8 Received signal levels relative to the clear weather median levels for rain during the night of April 6 - 7, 1987. Ku-band scaled from C-band using the bistatic radar equation and the frequency dependence of rain scatter.

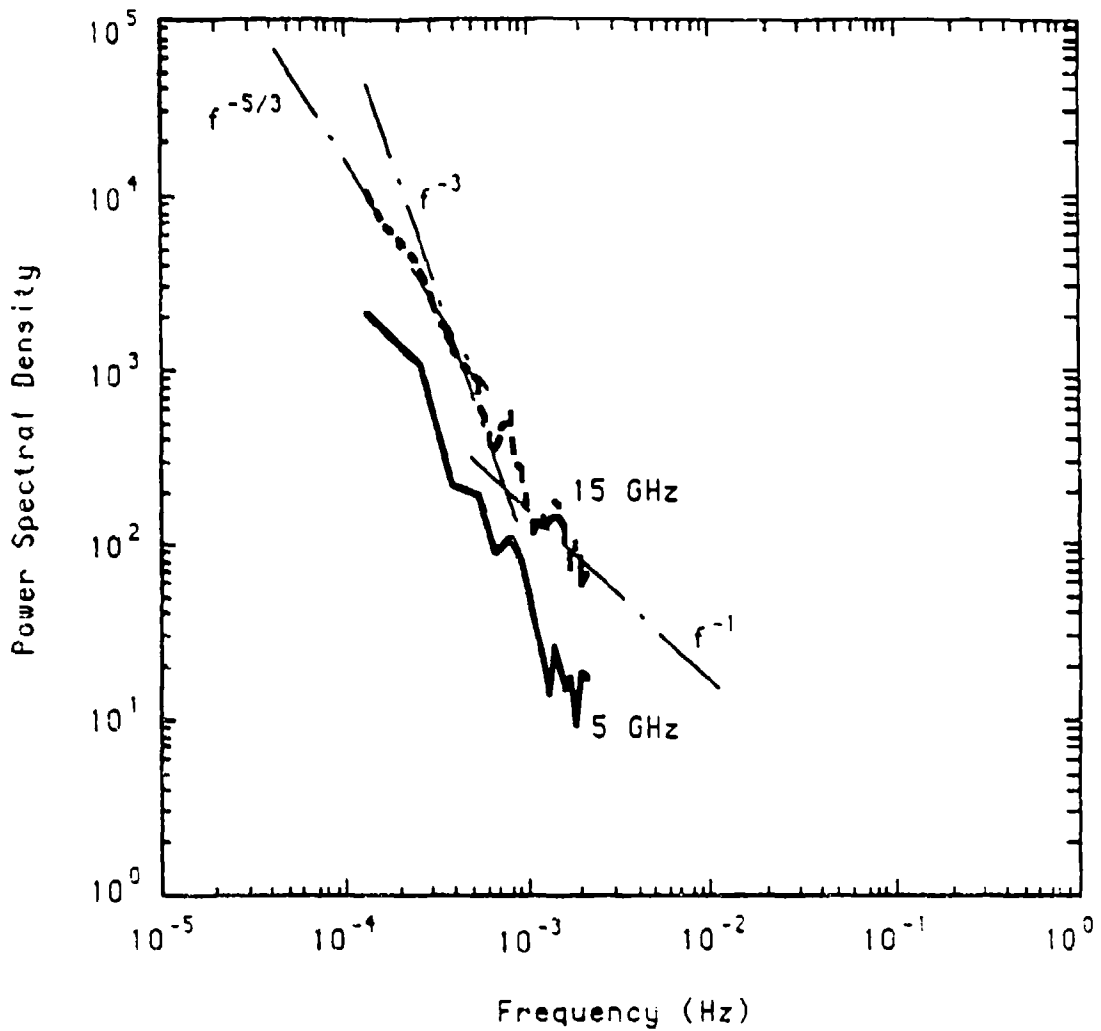


Figure 9 Power spectra for fluctuations in the logarithm of signal level (in dB) for a day with rain. Data are from Figure 7.

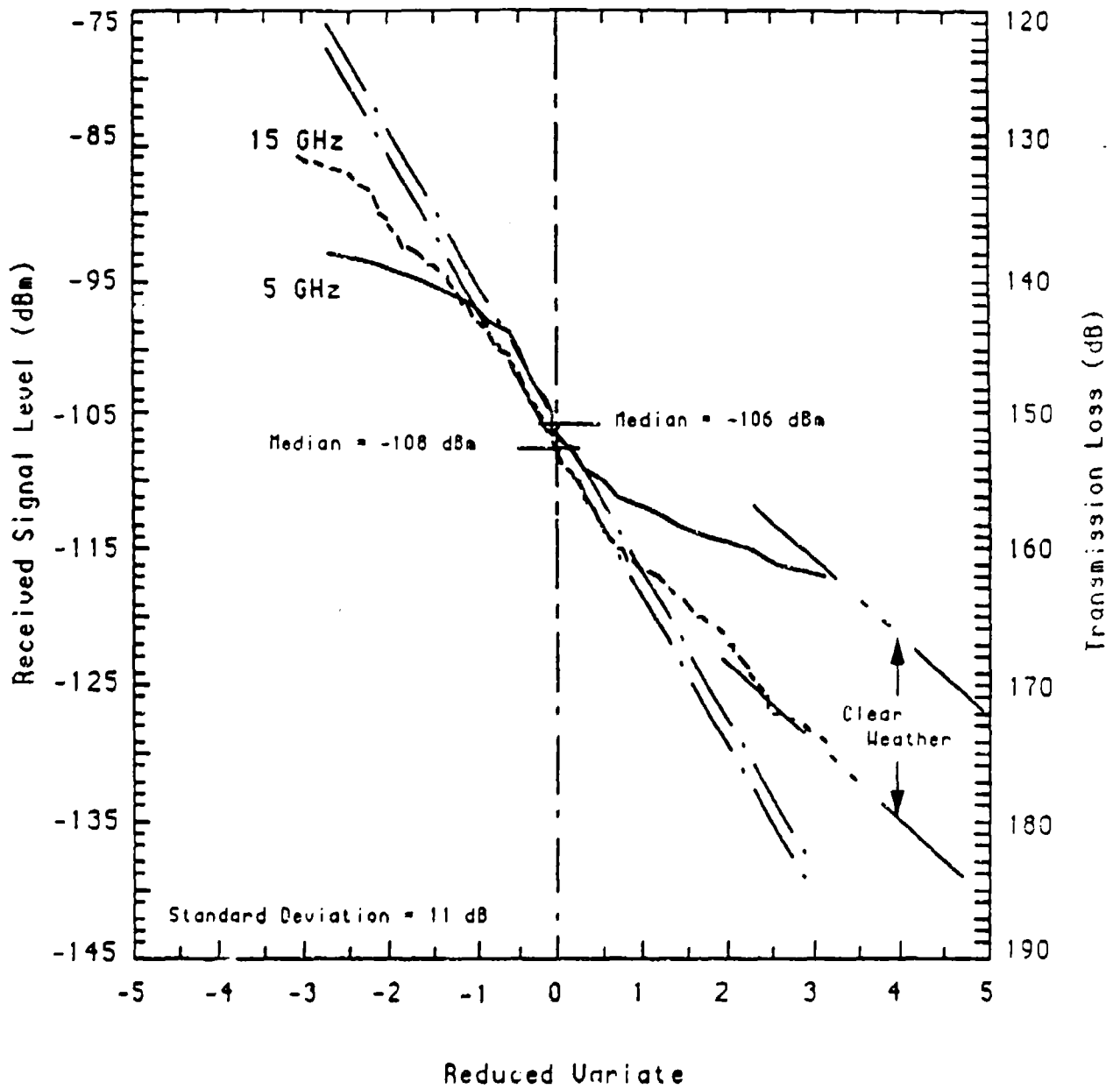


Figure 10 Cumulative signal level distribution for rainy conditions.

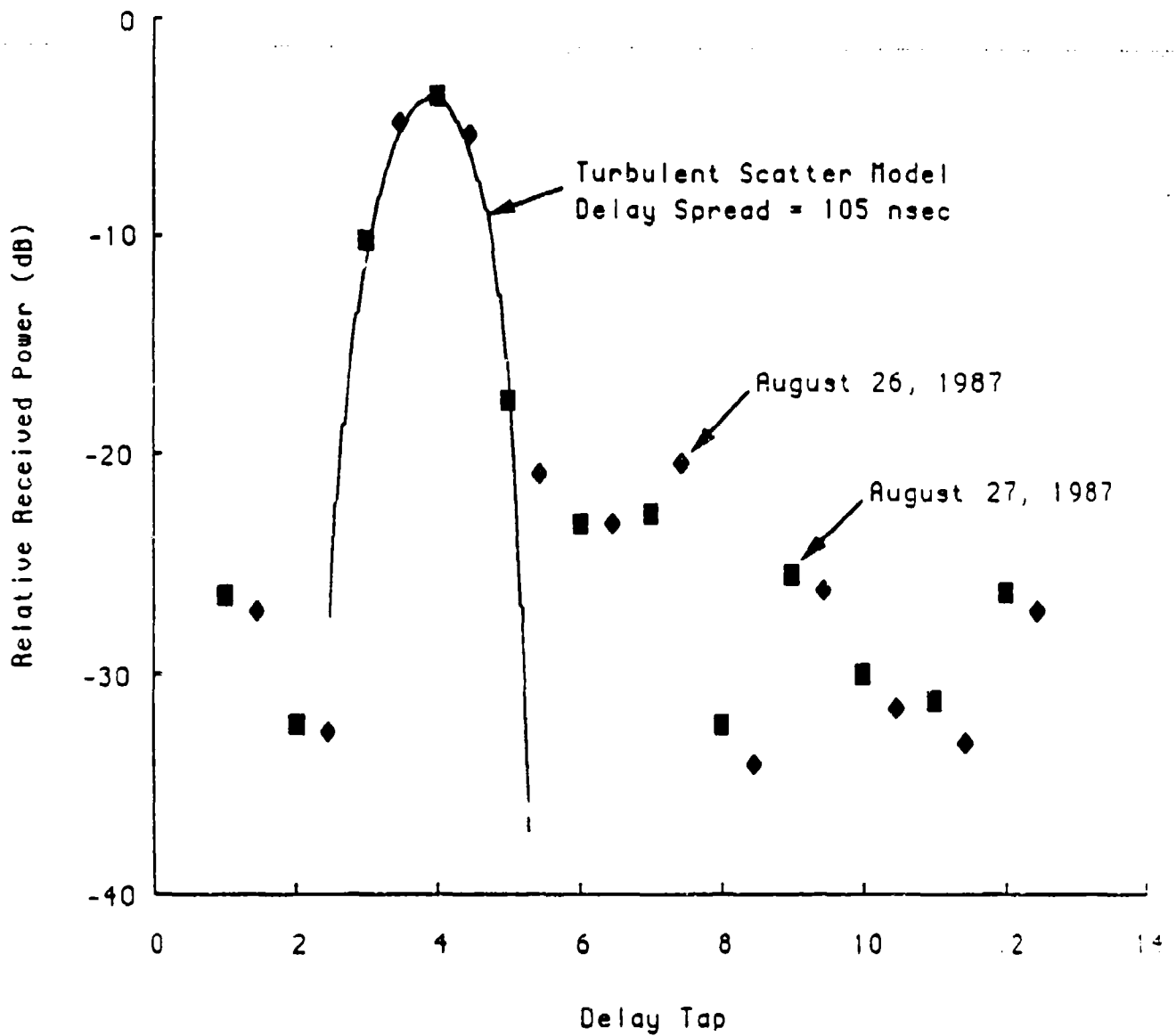


Figure 11 Average delay spread observations and model predictions for bistatic scattering from turbulence. Data are for periods with intermittent light rain. One tap or lag is equivalent to 80 nsec delay.

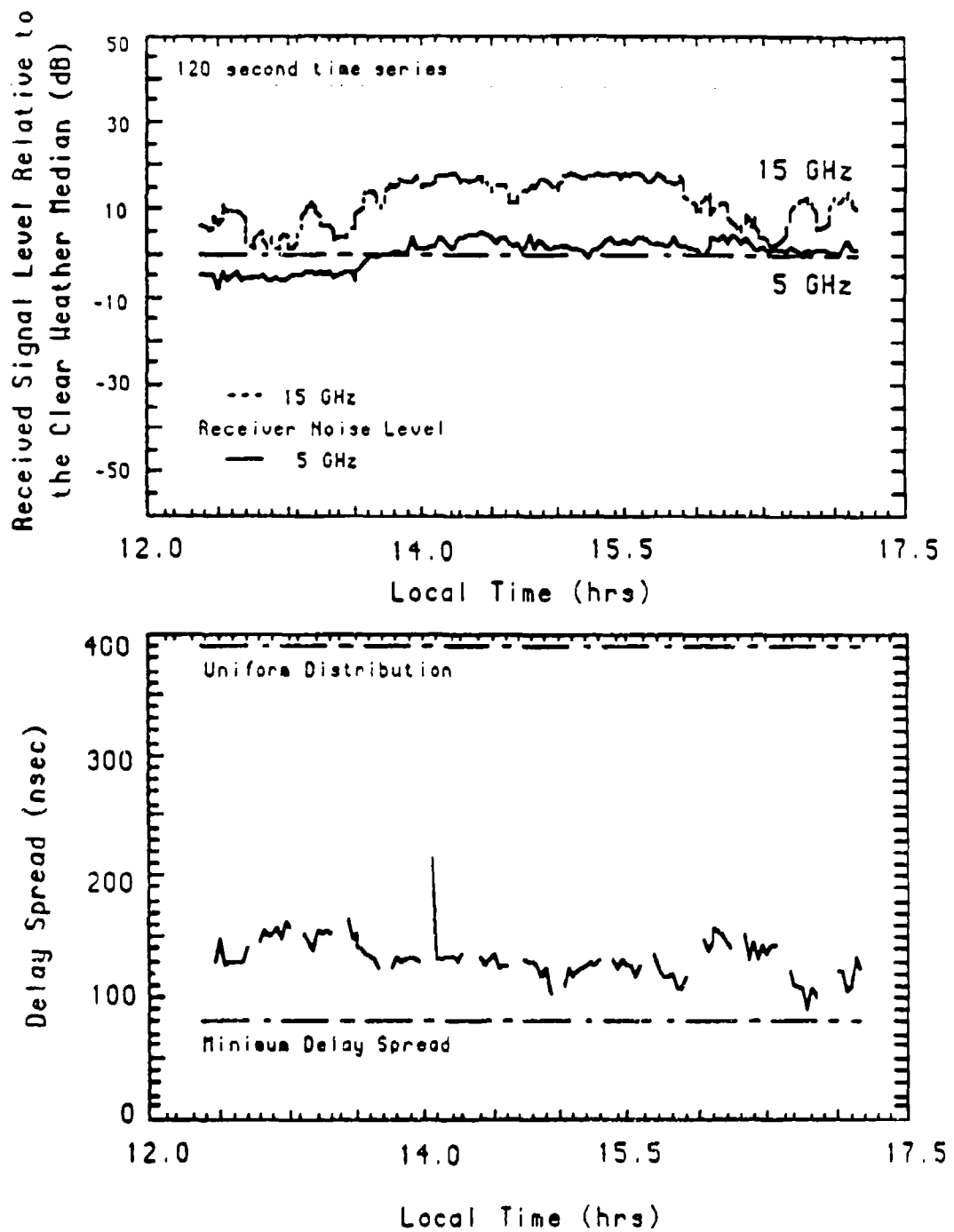


Figure 12 Received signal levels relative to the clear weather median values for rainy conditions on September 18, 1987 and delay spread measurements for the same time period.

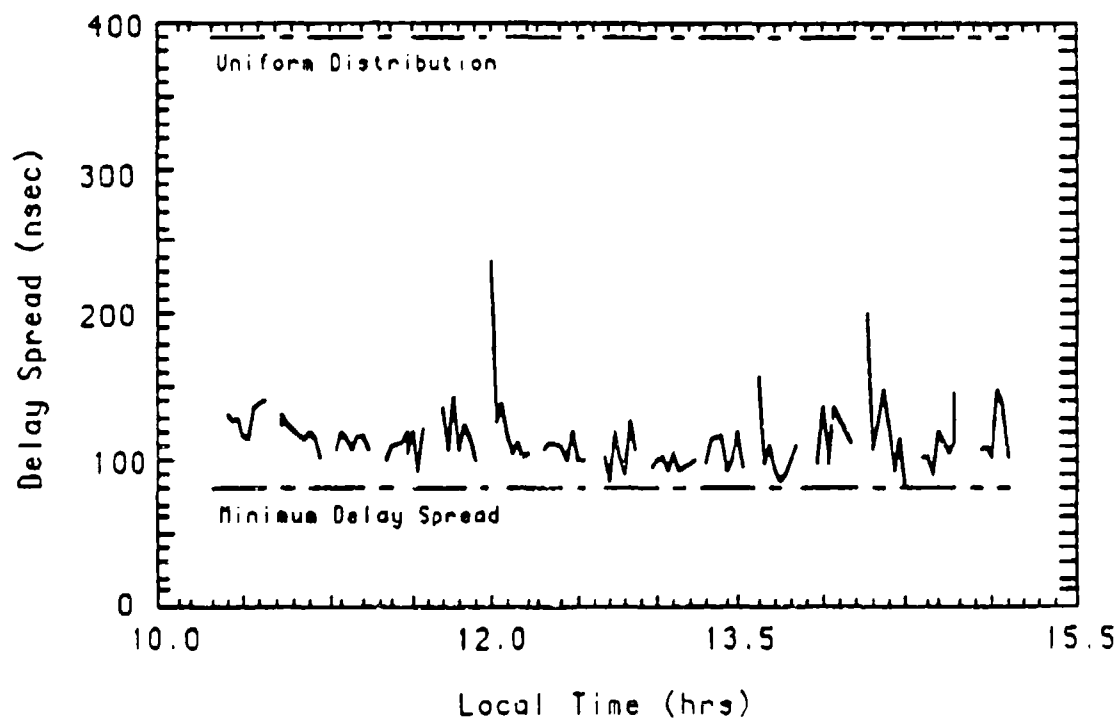
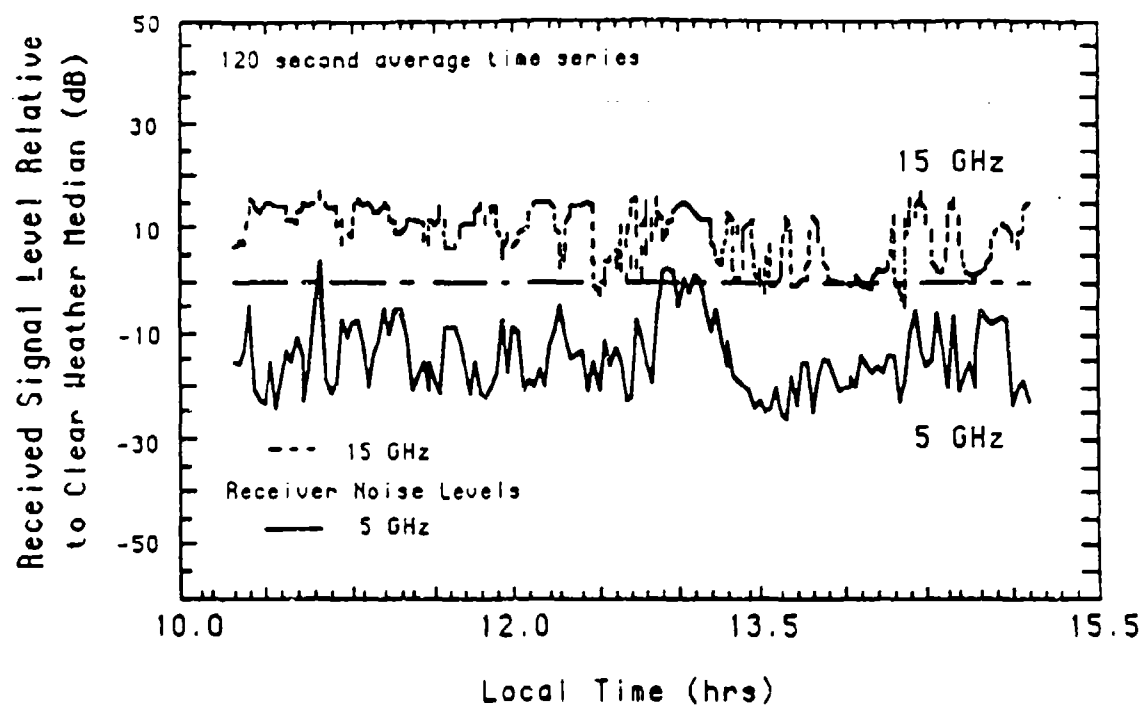


Figure 13 Signal levels relative to clear weather median values and delay spread at 15 GHz. Data are from clear weather conditions on August 26, 1986.

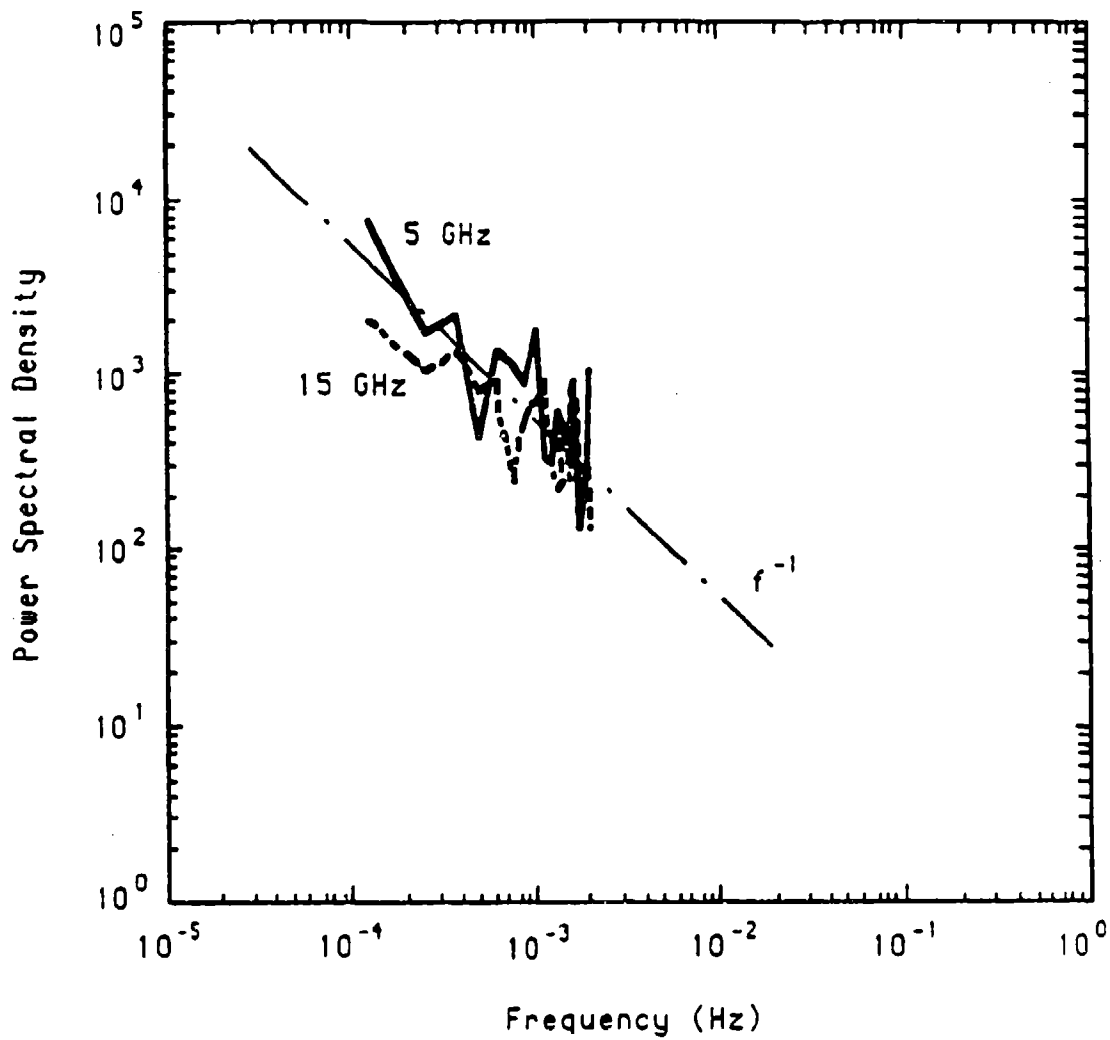
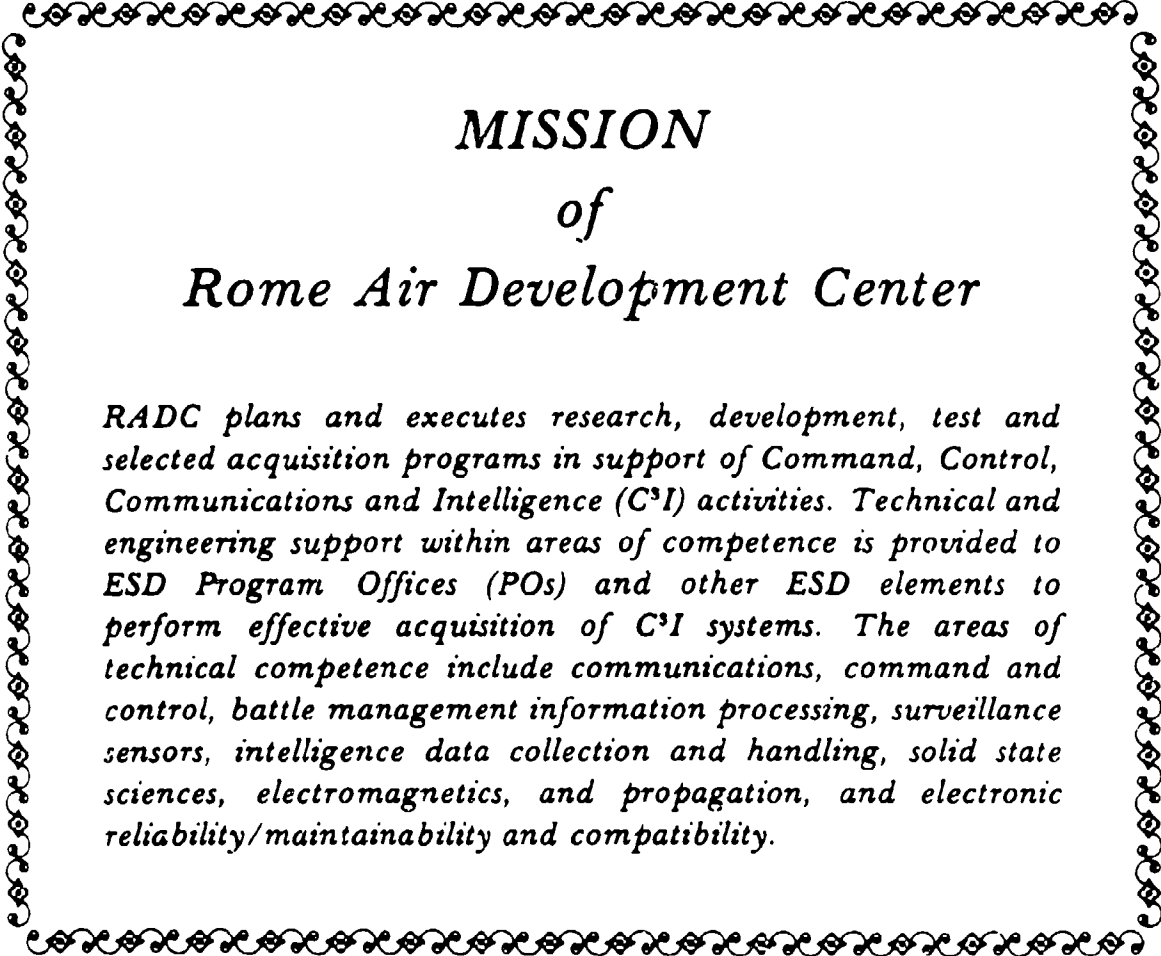


Figure 14 Power spectra for fluctuations in the logarithm of signal level (in dB) for a day with enhanced signal levels. Data are from Figure 13.



MISSION
of
Rome Air Development Center

RADC plans and executes research, development, test and selected acquisition programs in support of Command, Control, Communications and Intelligence (C³I) activities. Technical and engineering support within areas of competence is provided to ESD Program Offices (POs) and other ESD elements to perform effective acquisition of C³I systems. The areas of technical competence include communications, command and control, battle management information processing, surveillance sensors, intelligence data collection and handling, solid state sciences, electromagnetics, and propagation, and electronic reliability/maintainability and compatibility.